NASA Technical Memorandum 104606, Vol. 9

Technical Report Series on Global Modeling and Data Assimilation

Max J. Suarez, Editor

Volume 9

Energy and Water Balance Calculations in the Mosaic LSM

Randal D. Koster and Max J. Suarez

March 1996

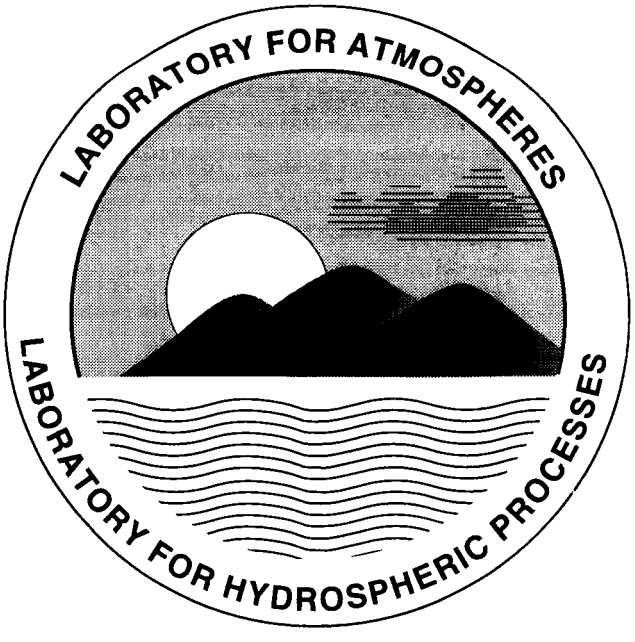

HYDROLOGICAL SCIENCES BRANCH

NASA Technical Memorandum 104606, Vol. 9

Technical Report Series on Global Modeling and Data Assimilation

Max J. Suarez, Editor
Goddard Space Flight Center
Greenbelt, Maryland

Volume 9

Energy and Water Balance Calculations in the Mosaic LSM

Randal D. Koster
Max J. Suarez
Goddard Space Flight Center
Greenbelt, Maryland

National Aeronautics and
Space Administration

Goddard Space Flight Center
Greenbelt, Maryland
1996

This publication is available from the NASA Center for AeroSpace Information,
800 Elkridge Landing Road, Linthicum Heights, MD 21090-2934, (301) 621-0390.

Abstract

The Mosaic land surface model (LSM), which is designed for use with an atmospheric general circulation model (GCM), computes areally-averaged energy and water fluxes from the land surface in response to meteorological forcing. The model allows explicit vegetation control over the computed surface energy and water balances, with environmental stresses (high temperatures, dry soil, etc.) acting to increase canopy resistance and thus decrease transpiration. The scheme includes a canopy interception reservoir and three soil reservoirs: a thin layer near the surface, a middle layer that encompasses the remainder of the root zone, and a lower "recharge" layer for long term storage. Bare soil evaporation, transpiration, and interception loss occur in parallel, and runoff occurs both as overland flow during precipitation events and as groundwater drainage out of the recharge layer. A complete snow budget is included. The model was originally derived from the SiB model of Sellers et al. (1986) and still maintains certain SiB formulations, particularly those for canopy resistance.

The model accounts for subgrid variability in surface characteristics through the "mosaic" approach. A grid square area containing several different vegetation regimes is divided into relatively homogeneous sub-regions ("tiles" of the mosaic), each containing a single vegetation or bare soil type. Observed vegetation distributions are used to determine the partitioning. A separate energy balance is calculated for each tile, and each tile maintains its own prognostic soil moisture contents and temperatures.

This report provides thorough documentation of the parameterizations used within a single Mosaic LSM tile. The requirements for coupling to a GCM are also discussed.

Contents

List of Figures

List of Tables

1 Introduction

The land surface model (LSM) described by Koster and Suarez (1992a) (hereafter referred to as the Mosaic LSM) has been fully coupled to the Aries GCM at NASA/GSFC, and the coupled models have been used to address a number of climate-related problems. For example, Koster and Suarez (1994) examined how simulated mean climate is affected by various components of the land surface, specifically those components that differentiate a surface-vegetation-atmosphere-transfer (SVAT) LSM from a typical bucket LSM. Koster and Suarez (1995) used the models to isolate the contributions of land and ocean processes to interannual precipitation variability, and Scott et al. (1995) used them in an analysis of land surface control over precipitation persistence. The Mosaic LSM is also incorporated into current simulations of the atmosphere/ocean/land system by GSFC's Coupled Climate Dynamics Group.

Although the Mosaic LSM was originally an offshoot of the Simple Biosphere, or SiB, LSM (Sellers et al. 1986), it has sufficiently diverged from SiB to warrant separate documentation. The present report describes the framework of the Mosaic LSM calculations (Section 2) and presents its specific energy and water balance formulations (Sections 3-6). The report ends with a detailed discussion of the model's coupling to the GCM (Section 7).

Three different versions of the Mosaic LSM are described in this report:

Version 1. This is the model version used by Koster and Suarez (1993, 1994, 1995). It is also the version used in PILPS, the Project for the Intercomparison of Land-surface Parameterization Schemes (Henderson-Sellers et al. 1993).

Version 2. This model, which was used by Scott et al. (1995, 1996), includes an improved formulation of the canopy interception reservoir.

Version 3. In addition to the improvements in Version 2, this model includes improved treatments of surface runoff and fractional snow cover, as well as a more comprehensive list of output variables.

For the most part, the three versions use identical physical parameterizations. The discussions below will mention version numbers only to distinguish version-specific features of the model.

2 Overview of Calculations

The Mosaic LSM is named for its use of the "mosaic" strategy to account for subgrid heterogeneity in surface characteristics. Using vegetation maps, every surface grid cell in the GCM is subdivided into relatively homogeneous subregions, or "mosaic tiles", each

tile containing a single vegetation or bare soil type (Koster and Suarez 1992a). Energy and water balance calculations are performed over each tile at every time step, and each tile maintains its own prognostic variables, i.e., its own moisture reservoir contents and temperatures. The tiles in a grid square respond to the mean conditions in the overlying GCM grid box; this grid box, in turn, responds to the areally-weighted fluxes of heat and moisture from the tiles. The tiles in a grid square do not interact with each other directly, though they can affect each other through the overlying atmosphere.

As the model is currently used in the GCM, a land surface tile can contain one of eight basic surface types: (1) broadleaf evergreen trees; (2) broadleaf deciduous trees; (3) needle-leaf trees; (4) grassland (groundcover); (5) broadleaf shrubs; (6) dwarf trees (tundra); (7) bare soil; and (8) desert soil. The model parameter values associated with each type are provided in Tables 1 through 10 of Appendix 2. Mixtures of vegetation types are not allowed within a tile; thus, a grid cell containing savanna would be split into two tiles, one containing trees and the other containing grass. As demonstrated by Koster and Suarez (1992b), the treatment of a homogeneous vegetation mixture as two isolated patches of vegetation generally has little effect on the average surface energy balance of the region. This method of treating homogeneous mixtures produces significant error only if the evaporation resistances imposed by the two types are extremely different.

The energy balance calculations performed by the Mosaic LSM within each tile are illustrated in Figure 1. A fraction of the incoming solar radiation is immediately reflected. The sum of absorbed solar radiation and downward longwave radiation is balanced by upwelling longwave radiation, outgoing latent heat, outgoing sensible heat, ground heat storage, and snowmelt. Canopy resistance, which controls transpiration rates, is allowed to vary with environmental stress. Heat transfer into the deep soil updates a deep soil temperature. A strict energy balance is maintained for the surface/canopy system and for the deep soil at every time step; energy is never created or destroyed, except possibly through numerical round-off.

The water balance calculations performed within each tile are illustrated in Figure 2. Of the precipitation water falling on the land surface, some is added to a canopy interception reservoir, which accounts for the ability of leaves and ground litter to hold small amounts of "free-standing" water from which evaporation occurs unhindered. The rest of the precipitation falls through to the soil surface, and this throughfall is in turn partitioned into surface runoff (overland flow) and infiltration into the shallow surface soil layer. Water diffuses between the surface soil layer and a second soil layer, which encompasses the remainder of the root zone. Water also diffuses between the root layer and a third, larger soil layer that allows long-term storage of soil moisture, and water can percolate out of this third layer and thus out of the modeled soil column. Evaporation extracts moisture from the interception reservoir, from the top two soil layers, and from any snowpack present. (Though not shown in Figure 2, a snow budget is included.) The Mosaic LSM ensures a strict water balance for every surface reservoir. Only numerical round-off can create or destroy water mass.

Each land surface tile has eight prognostic variables. Three are associated with the energy

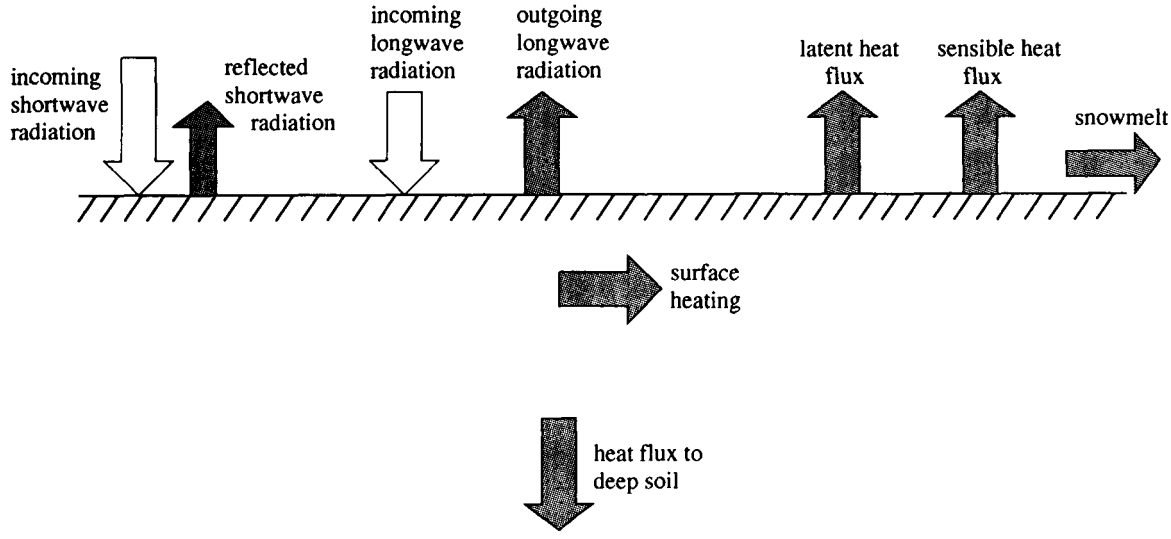

Figure 1: The energy balance at the land surface. The shaded fluxes are computed within the Mosaic LSM; the others are provided by the GCM.

balance equations:

T_c, the temperature of the surface/canopy system,

T_d, the temperature deep in the soil, and

e_a, the vapor pressure in the canopy air.

Five are associated with the water balance equations:

C, the moisture content of the canopy interception reservoir,

W_1, the moisture content of the top soil layer,

W_2, the moisture content of the middle soil layer,

W_3, the moisture content of the bottom soil layer, and

S, the moisture held within the snowpack, if any.

These prognostic variables are updated at every time step.

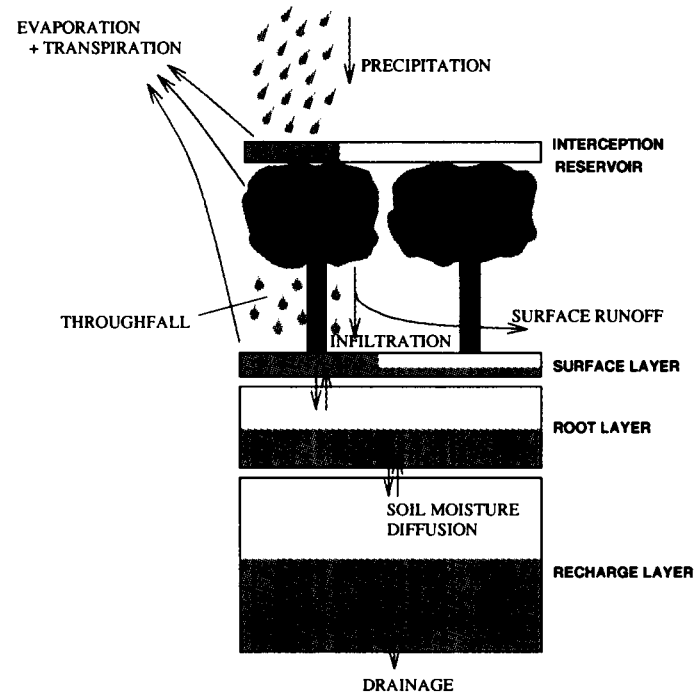

Figure 2: Schematic of the water balance calculations performed by the Mosaic LSM.

3 Energy Balance: Solution Procedure

The surface energy fluxes are computed at each time step by solving two equations simultaneously at each land surface tile: one for the surface energy balance itself, and one that equates vapor transport into the canopy air with vapor transport away from the canopy air. The present section describes how these two equations are set up and solved. Section 4 will describe how the individual components of the equations are computed.

3.1 Surface Energy Balance Equation

The surface energy balance equation, in the absence of snowmelt, is

$$R_{\mathrm{sw-net}} + R_{\mathrm{lw}}^{\downarrow} = \frac{C_H \delta T_c}{\Delta t} + R_{\mathrm{lw}}^{\uparrow} + H + \lambda E + G_D, \tag{1}$$

where

$R_{\mathrm{sw-net}}$ = net shortwave radiation absorbed at the surface,
$R_{\mathrm{lw}}^{\downarrow}$ = longwave radiation absorbed at the surface,
C_H = heat capacity associated with surface/canopy system,
δT_c = change in surface-canopy temperature, T_c, over time step,

Δt = time step duration,
$R_{\text{lw}}^{\uparrow}$ = upward longwave radiation at surface,
H = sensible heat flux,
λ = latent heat of vaporization,
E = evaporation rate, and
G_D = heat flux to deep soil.

Energy associated with snowmelt is treated separately, as outlined in Section 3.4.

Each of the energy fluxes in (1) is assumed consistent with the *updated* surface temperature, T_c, and canopy air vapor pressure, e_a, for the time step. Because these updated values are not known a priori when the energy balance is calculated (i.e., because an implicit solution is desired), the Mosaic LSM uses the following linearizations:

$$R_{\text{lw}}^{\uparrow} = \left[R_{\text{lw}}^{\uparrow}\right]_{\text{old}} + \left[\frac{dR_{\text{lw}}^{\uparrow}}{dT_c}\right]_{\text{old}} \delta T_c, \tag{2}$$

$$H = [H]_{\text{old}} + \left[\frac{\partial H}{\partial T_c}\right]_{\text{old}} \delta T_c + \left[\frac{\partial H}{\partial e_a}\right]_{\text{old}} \delta e_a, \tag{3}$$

$$E = [E]_{\text{old}} + \left[\frac{\partial E}{\partial T_c}\right]_{\text{old}} \delta T_c + \left[\frac{\partial E}{\partial e_a}\right]_{\text{old}} \delta e_a, \tag{4}$$

and

$$G_D = [G_D]_{\text{old}} + \left[\frac{dG_D}{dT_c}\right]_{\text{old}} \delta T_c, \tag{5}$$

where the subscript "old" denotes quantities calculated using the previous time step's values of T_c and e_a, and where δT_c and δe_a are the changes in the surface temperature and canopy vapor pressure, respectively, that occur over the time step. With these linearizations, the energy balance can be rewritten as

$$R_{\text{sw-net}} + R_{\text{lw}}^{\downarrow} - \left[R_{\text{lw}}^{\uparrow} + H + \lambda E + G_D\right]_{\text{old}} =$$

$$\left[\frac{C_H}{\Delta t} + \frac{dR_{\text{lw}}^{\uparrow}}{dT_c} + \frac{\partial H}{\partial T_c} + \lambda\frac{\partial E}{\partial T_c} + \frac{dG_D}{dT_c}\right]_{\text{old}} \delta T_c + \left[\frac{\partial H}{\partial e_a} + \lambda\frac{\partial E}{\partial e_a}\right]_{\text{old}} \delta e_a. \tag{6}$$

Mosaic LSM Versions 1 and 2 differ from Version 3 in the value of λ used when snow is present. In Versions 1 and 2, the presence of snow implies that the only evaporation possible is snow sublimation, and λ is set to the latent heat of sublimation. In Version 3, evaporation can occur in parallel from the snowpack and from the snow-free fraction of the land surface tile. In Version 3, λ is set to

$$\lambda = f_{\text{E-snow}}\lambda_s + (1 - f_{\text{E-snow}})\lambda_e, \tag{7}$$

where λ_s is the latent heat of sublimation, λ_ϵ is the latent heat of vaporization of liquid water, and $f_{\text{E-snow}}$ is the ratio of snow sublimation to total evaporation, which can be determined before the evaporation itself is calculated, using (114). (See Section 6.3.2.)

3.2 Vapor Flux Equation

Equation (6) has two unknowns, δT_c and δe_a, and thus another equation is needed. For the second equation, the Mosaic LSM assumes that the canopy air has negligible storage capacity for water vapor, so that the flux of moisture from the trees and soil into the canopy air, E_{surf}, is exactly balanced by the flux out of the canopy into the overlying atmosphere, E, as calculated with (4). E_{surf} is computed with:

$$E_{\text{surf}} = \frac{\rho\epsilon}{p_s} \frac{(e_s(T_c) - e_a)}{r_{\text{eff}}}, \tag{8}$$

where ρ is air density, ϵ is the ratio of the molecular weight of water vapor to that of dry air, p_s is the surface pressure, $e_s(T_c)$ is the saturated vapor pressure at the temperature T_c, and r_{eff} is the effective surface resistance to vapor transport, which varies with T_c and e_a. By linearizing (8) around $[T_c]_{\text{old}}$ and $[e_a]_{\text{old}}$ and combining with (4), the equation $E = E_{\text{surf}}$ is transformed into:

$$\begin{aligned} &[\,(E - E_{\text{surf}})\, r_{\text{eff}}\,]_{\text{old}} \quad = \\ &\left[-r_{\text{eff}} \frac{\partial E}{\partial T_c} + \frac{\rho\epsilon}{p_s} \frac{\partial e_s}{\partial T_c} - E_{\text{H}} \frac{\partial r_{\text{eff}}}{\partial T_c}\right]_{\text{old}} \delta T_c \\ &- \left[r_{\text{eff}} \frac{\partial E}{\partial e_a} + \frac{\rho\epsilon}{p_s} + E_{\text{H}} \frac{\partial r_{\text{eff}}}{\partial e_a}\right]_{\text{old}} \delta e_a, \end{aligned} \tag{9}$$

where E_{H} is the harmonic mean of $[E]_{\text{old}}$ and $[E_{\text{surf}}]_{\text{old}}$. In fact, E_{H} in (9) could be replaced by either $[E]_{\text{old}}$ or $[E_{\text{surf}}]_{\text{old}}$, depending on the order in which the terms are linearized. The harmonic mean is used to increase the calculation's stability.

Stability is further increased by requiring that

$$\left[\frac{\rho\epsilon}{p_s} \frac{\partial e_s}{\partial T_c} - E_{\text{H}} \frac{\partial r_{\text{eff}}}{\partial T_c}\right]_{\text{old}} > 0. \tag{10}$$

and

$$\left[\frac{\rho\epsilon}{p_s} + E_{\text{H}} \frac{\partial r_{\text{eff}}}{\partial e_a}\right]_{\text{old}} > 0. \tag{11}$$

If either sum is negative, it is reset to zero before (9) is used. The idea is to ensure that the indirect changes in evaporation associated with changes in canopy resistance do not exceed the more direct changes associated with changes in e_a and T_c.

Equation (9) is modified when the surface resistance is zero, e.g., due to the presence of snow (in Versions 1 and 2) or a saturated canopy (see Section 4.4). Under these conditions, the canopy air vapor pressure, e_a, is assumed equal to $e_s(T_c)$, so that (9) is replaced with:

$$[e_s(T_c) - e_a]_{\text{old}} = -\frac{\partial e_s}{\partial T_c} \delta T_c + \delta e_a \tag{12}$$

In fact, substituting (8) into (9) and setting r_{eff} and its derivatives to zero produces (12) exactly.

3.3 Solution of Simultaneous Equations

The Mosaic LSM solves (6) and (9) (or solves (6) and (12), in the case of zero surface resistance) to produce values of δT_c and δe_a for the time step. This allows the calculation of the sensible heat flux and evaporation rate for the time step, using (3) and (4). It also allows the updating of the prognostic variables T_c and e_a:

$$[T_c]_{\text{new}} = [T_c]_{\text{old}} + \delta T_c \tag{13}$$

$$[e_a]_{\text{new}} = [e_a]_{\text{old}} + \delta e_a \tag{14}$$

Before the prognostic variables are updated, though, several checks are made on the calculated fluxes. First, the Mosaic LSM ensures that sufficient water is available for the calculated evaporation rate. The available water, W_{avail}, is calculated in Versions 1 and 2 as

$$W_{\text{avail}} = \begin{cases} C + W_1 + W_2, & \text{when snow is not present} \\ S, & \text{when snow is present} \end{cases} \tag{15}$$

and in Version 3 as

$$W_{\text{avail}} = C + W_1 + W_2 + S. \tag{16}$$

If the calculated evaporation for the time step, $E\Delta t$, is greater than W_{avail}, then all available water evaporates during the time step, and the canopy air vapor pressure, e_a, is reset to the GCM-provided vapor pressure in the overlying air, e_m. The value of δT_c is then recomputed using (6) alone, after setting both $\left[\frac{\partial E}{\partial T_c}\right]_{\text{old}}$ and $\left[\frac{\partial E}{\partial e_a}\right]_{\text{old}}$ to zero, replacing δe_a by $e_m - e_a$, and replacing λE by $\lambda W_{\text{avail}}/\Delta t$. The sensible heat flux is computed using (3) with the modified δT_c.

Second, the Mosaic LSM checks that the calculated evaporation rate is consistent with the vapor pressure gradients. A positive flux in the presence of a newly-established negative gradient (or vice-versa) is possible under certain conditions as a result of the linearizations used in the solution procedure. Also, the terms $\left[\frac{\partial E}{\partial T_c}\right]_{\text{old}}$ and $\left[\frac{\partial E}{\partial e_a}\right]_{\text{old}}$ are untrustworthy when the calculated evaporation and $[E]_{\text{old}}$ have opposite sign. Such cases are rare, but when they occur, the Mosaic LSM sets the evaporation rate to zero and sets δe_a to $e_m - e_a$, i.e., it sets the canopy vapor pressure to the vapor pressure in the overlying air. It then uses (6) alone to recompute δT_c, after resetting λE, $\left[\frac{\partial E}{\partial T_c}\right]_{\text{old}}$ and $\left[\frac{\partial E}{\partial e_a}\right]_{\text{old}}$ to zero. The sensible heat flux is recomputed using the modified δT_c.

Finally, the Mosaic LSM puts a limit on the computed δe_a — if δe_a is too large, the assumed linearizations are invalid, and an instability may develop. (Such problems are less likely with δT_c, since temperature change is mitigated by the surface's heat capacity.) When (6) and (9) are used to compute δT_c and δe_a, with no modification, δe_a is constrained to have a magnitude no greater than $e_a/2$. If δe_a is indeed reset through this constraint, δT_c is recomputed using (6) alone, using the newly prescribed value of δe_a. Surface fluxes are adjusted accordingly, using (3) and (4).

3.4 Correction for Snowmelt

If snow is present on the surface at the beginning of a time step, and if the computed T_c at the end of the time step is above the freezing point, T_f (=273.16K), then snowmelt is assumed to occur, and the energy balance must be recomputed. The approach used in Versions 1 and 2 differs slightly from that used in Version 3.

a. *Versions 1 and 2.* The assumed new values of δT_c and δe_a are

$$\delta T_c = T_f - [T_c]_{\text{old}} \tag{17}$$

and

$$\delta e_a = \frac{\partial e_s}{\partial T_c} \delta T_c. \tag{18}$$

Equation (17) resets T_c to T_f. The outgoing longwave radiation, sensible heat flux, evaporation rate, and ground heating are recomputed with (2) through (5). The rate of snowmelt, S_{melt}, is computed by dividing the residual energy available for melting (calculated with the new values of δT_c and δe_a) by the latent heat of fusion, λ_f:

$$S_{\text{melt}} = \frac{\left[R_{\text{sw-net}} + R^{\downarrow}_{\text{lw}} - \frac{C_H \delta T_c}{\Delta t} - R^{\uparrow}_{\text{lw}} - H - \lambda E - G_D\right]_{\text{new}}}{\lambda_f}. \tag{19}$$

At times, the entire snowpack will melt during the time step, with enough energy left over to heat the surface above T_f. This is not allowed by the snowmelt formulation in Versions 1 and 2, which for convenience always resets T_c to T_f when snowmelt occurs. To maintain a strict energy balance in this situation, the residual energy that remains after melting all of the snow is arbitrarily added to the sensible heat flux. Thus, for this particular time step, the sensible heat flux is artificially high.

b. *Version 3.* The energy balance is first recalculated under the extreme assumption that all the snow has melted. Equation (6) is rewritten as:

$$R_{\text{sw-net}} + R^{\downarrow}_{\text{lw}} - \left[R^{\uparrow}_{\text{lw}} + H + \lambda E + G_D\right]_{\text{old}} - \lambda_f \left(\frac{[S]_{\text{old}} - E_{\text{snow}} \Delta t}{\Delta t}\right) =$$

$$\left[\frac{C_H}{\Delta t} + \frac{dR^{\uparrow}_{\text{lw}}}{dT_c} + \frac{\partial H}{\partial T_c} + \lambda \frac{\partial E}{\partial T_c} + \frac{dG_D}{dT_c}\right]_{\text{old}} \delta T_c + \left[\frac{dH}{de_a} + \lambda \frac{\partial E}{\partial e_a}\right]_{\text{old}} \delta e_a. \tag{20}$$

where S is the snow mass and E_{snow} is the evaporation rate from snow, calculated with (115). Equations (20) and (9) are then solved simultaneously for δT_c and δe_a.

If, in fact, only a fraction of the snow should melt (the most common condition), $[T_c]_{\text{old}}$ plus this new value of δT_c will lie below T_f, and the energy balance must be computed still another time. The value of $[T_c]_{\text{new}}$ is set to T_f, using (17), and δe_a is computed with (9) and (17). The amount of snowmelt is then computed with (19).

Version 3 thus differs from Versions 1 and 2 in that it allows the ground to heat above T_f and updates e_a in a more sensible way.

3.5 Energy Balance in the Deep Soil

The deep soil temperature, T_d, is not updated implicitly. Once $[T_c]_{\text{new}}$ is known, $[T_d]_{\text{new}}$ is computed as

$$[T_d]_{\text{new}} = [T_d]_{\text{old}} + G_D \Delta t / C_{\text{H-deep}}, \tag{21}$$

where $C_{\text{H-deep}}$ is the heat capacity associated with the deep soil, and where G_D is calculated with (5). The values used in the T_d calculation are consistent with the force-restore equations of Deardorf (1978); see Section 4.7 below.

4 Energy Balance: Components

Several of the terms in the two equations for δT_c and δe_a, (6) and (9), are provided by the GCM. For example, the GCM provides the downwelling longwave radiation, $R_{\text{lw}}^{\downarrow}$. Also, because the GCM is assumed to perform all of the boundary layer transport calculations, it is expected to provide values for $[E]_{\text{old}}$, $[\frac{\partial E}{\partial T_c}]_{\text{old}}$, $[\frac{\partial E}{\partial e_a}]_{\text{old}}$, $[H]_{\text{old}}$, $[\frac{\partial H}{\partial T_c}]_{\text{old}}$, and $[\frac{dH}{de_a}]_{\text{old}}$, using the values of T_c and e_a provided by the LSM at the end of the previous time step. The LSM modifies the derivatives only when they appear unrealistic — $[\frac{\partial E}{\partial T_c}]_{\text{old}}$, $[\frac{dH}{de_a}]_{\text{old}}$, $[\frac{\partial E}{\partial e_a}]_{\text{old}}$, and $[\frac{\partial H}{\partial T_c}]_{\text{old}}$ are forced to lie at or above certain critical values, as necessary for the stability of the energy balance calculations.

The GCM also supplies values for $e_s([T_c]_{\text{old}})$ and $[\frac{\partial e_s}{\partial T_c}]_{\text{old}}$ in order to ensure consistency between the GCM and LSM phase change calculations. The Aries GCM currently provides these values only for the liquid/vapor transition, even for sub-freezing temperatures. As a result, snow sublimation rates in the coupled system may be slightly overestimated. The Aries GCM is now being modified to provide $e_s([T_c]_{\text{old}})$ and $[\frac{\partial e_s}{\partial T_c}]_{\text{old}}$ for the solid/vapor transition when T_c lies below the freezing point.

The formulations used at each land surface tile for the remaining terms in the energy balance equations are discussed in the present section. The calculation of $R_{\text{sw-net}}$ in (6) requires the assignment of surface reflectances (Section 4.1). The determination of r_{eff}, $\frac{\partial r_{\text{eff}}}{\partial T_c}$, $\frac{\partial r_{\text{eff}}}{\partial e_a}$, and E_{surf} (and thus E_{H}) in (9) is a rather lengthy process that is described in Sections 4.2 through 4.5. The linearization of the upward longwave radiation (terms $[R_{\text{lw}}^{\uparrow}]_{\text{old}}$ and $[\frac{dR_{\text{lw}}^{\uparrow}}{dT_c}]_{\text{old}}$) is discussed in Section 4.6, and the deep soil heat flux calculation (terms $[G]_{\text{old}}$ and $[\frac{dG}{dT_c}]_{\text{old}}$) is discussed in Section 4.7.

4.1 Surface Reflectance

Solar radiation must be separated by the GCM into four components: visible direct radiation ($R_{\mathrm{v-dir}}$); visible diffuse radiation ($R_{\mathrm{v-dif}}$); near-infrared direct radiation ($R_{\mathrm{ni-dir}}$); and near-infrared diffuse radiation ($R_{\mathrm{ni-dif}}$). The land surface model computes an albedo ($\alpha_{\mathrm{v-dir}}$, $\alpha_{\mathrm{v-dif}}$, $\alpha_{\mathrm{ni-dir}}$, and $\alpha_{\mathrm{ni-dif}}$) for each component. This allows the calculation of the net shortwave radiation at the surface:

$$R_{\mathrm{sw-net}} = (1-\alpha_{\mathrm{v-dir}})R_{\mathrm{v-dir}} + (1-\alpha_{\mathrm{v-dif}})R_{\mathrm{v-dif}} + (1-\alpha_{\mathrm{ni-dir}})R_{\mathrm{ni-dir}} + (1-\alpha_{\mathrm{ni-dif}})R_{\mathrm{ni-dif}}. \quad (22)$$

In addition to varying with vegetation type, the reflectances vary seasonally with leaf area index and greenness fraction, and they vary diurnally with the solar zenith angle. The algorithm used is an approximation to the full two-stream calculations of SiB, though with a slight improvement in the calculation of the diffuse reflectances. Full details are provided by Koster and Suarez (1991).

The presence of snow increases surface reflectance and thus decreases $R_{\mathrm{sw-net}}$. In Versions 1 and 2, a simple ramping function is used to convert the reflectance associated with vegetation to a reflectance associated with a vegetation-snow mixture. If $\alpha_{\mathrm{veg,v-dir}}$ is the surface reflectance for visible direct radiation in the absence of snow, and if $\alpha_{\mathrm{snow,v-dir}}$ is the corresponding reflectance over complete snow cover, then the net reflectance for visible direct radiation is computed as:

$$\alpha_{\mathrm{v-dir}} = \begin{cases} \alpha_{\mathrm{veg,v-dir}}, & S < S_{\mathrm{crit1}} \\ \alpha_{\mathrm{veg,v-dir}} + (\alpha_{\mathrm{snow,v-dir}} - \alpha_{\mathrm{veg,v-dir}})\frac{S-S_{\mathrm{crit1}}}{S_{\mathrm{crit2}}-S_{\mathrm{crit1}}}, & S_{\mathrm{crit1}} < S < S_{\mathrm{crit2}} \\ \alpha_{\mathrm{snow,v-dir}}, & S_{\mathrm{crit2}} < S, \end{cases} \quad (23)$$

where S is the snow mass and S_{crit1} and S_{crit2} are vegetation-dependent critical snow amounts. Corresponding equations are used for the reflectances of the other three shortwave radiation components.

Due to an error in the implementation of this ramping function, S_{crit1} and S_{crit2} were set to excessively low values, implying an essentially discontinuous jump in reflectance when going from snow-free to snow conditions. This discontinuity is present in the coupled GCM/LSM simulations using Versions 1 and 2. The error was corrected, however, before Version 1 was used in the PILPS intercomparison project (Henderson-Sellers et al. 1993).

Version 3 of the Mosaic LSM uses a different ramping function:

$$\alpha_{\mathrm{v-dir}} = \alpha_{\mathrm{veg,v-dir}} + (\alpha_{\mathrm{snow,v-dir}} - \alpha_{\mathrm{veg,v-dir}})\frac{S}{S+S_{\mathrm{mid}}}, \quad (24)$$

where S_{mid} is a vegetation-dependent parameter. (Again, corresponding equations are used for the other shortwave radiation components.) This formulation is similar to that used in BATS (Dickinson et al. 1986).

4.2 Canopy Resistance

The canopy resistance, r_c, is the resistance provided by vegetation stomata to transpiration, E_T:

$$E_T = \frac{\rho\epsilon}{p_s}\frac{(e_s(T_c) - e_a)}{r_c}. \tag{25}$$

The canopy resistance calculation requires two steps: (1) the determination of an unstressed canopy resistance, a function only of vegetation type and incoming photosynthetically active radiation (PAR), and (2) the incorporation of stress terms that increase the resistance when the vegetation experiences non-optimal environmental conditions. As discussed in Section 4.4, (25) is not used directly in the energy balance calculations. Instead, r_c is combined with the resistances for bare soil evaporation and interception loss to produce a net effective resistance, r_{eff}, for the surface.

4.2.1 Unstressed Canopy Resistance

The formulation of unstressed resistance, $r_{\text{c-unstressed}}$, is taken directly from the SiB LSM formulation (Sellers et al. 1986). The unstressed canopy resistance function at the bottom of Table 4 in Sellers (1985) is:

$$\frac{1}{r_{\text{c-unstressed,green}}} =$$

$$\frac{1}{kc}\left[\frac{b}{F_o d}\ln\left(\frac{\mu d e^{kL_t} + G(\mu)}{\mu d + G(\mu)}\right) - \ln\left(\frac{\mu d + G(\mu)e^{-kL_t}}{\mu d + G(\mu)}\right)\right], \tag{26}$$

where

$$d = \frac{a + bc}{cF_o}, \tag{27}$$

and where a, b, and c are constants describing the resistance to transpiration provided by a single stomate (see equation (17) in Sellers (1985)), F_o is the sum of the visible direct and visible diffuse components of the incoming solar radiation (i.e., the PAR flux, provided by the GCM), k is an extinction coefficient, L_t is the leaf area index, μ is the cosine of the solar zenith angle (provided by the GCM), and $G(\mu)$ is the relative projected area of leaf elements in the direction of this angle. This equation represents the integral of the resistance function for a single stomate across a vegetation canopy that is assumed to consist only of live (green) leaves. Note that (26) can be rewritten as

$$\frac{1}{r_{\text{c-unstressed,green}}} = \frac{1}{kc}\left[kL_t + \left(\frac{b}{F_o d} - 1\right)\ln\left(\frac{\frac{\mu d e^{kL_t}}{G(\mu)} + 1}{\frac{\mu d}{G(\mu)} + 1}\right)\right]. \tag{28}$$

Because the solar radiation has both direct and diffuse components, and because (28) applies only to direct radiation, the term $G(\mu)/\mu$ is replaced by a different function, Ψ:

$$\frac{1}{r_{\text{c-unstressed,green}}} = \frac{1}{kc}\left[kL_t + \left(\frac{b}{F_o d} - 1\right)\ln\left(\frac{\frac{de^{kL_t}}{\Psi} + 1}{\frac{d}{\Psi} + 1}\right)\right], \tag{29}$$

where Ψ is a weighted average of two functions, one for direct radiation ($G(\mu)/\mu$) and one for diffuse radiation (Ψ_{dif}):

$$\Psi = f_{\text{dir}}\frac{G(\mu)}{\mu} + (1 - f_{\text{dir}})\Psi_{\text{dif}}, \tag{30}$$

where f_{dir} is the ratio of direct solar radiation to total solar radiation. Following Sellers (1985),

$$G(\mu) = \phi_1 + \phi_2\mu, \tag{31}$$

where

$$\phi_1 = 0.5 - 0.633\chi_L - 0.33{\chi_L}^2, \tag{32}$$

$$\phi_2 = 0.877(1 - 2\phi_1), \tag{33}$$

and χ_L describes the departure of leaf angles from a spherical distribution. The equation used for Ψ_{dif} was not provided by Sellers (1985) or Sellers et al. (1986) and was thus extracted from the SiB computer code itself:

$$\Psi_{\text{dif}} = \phi_2(\frac{1}{3} + \frac{\pi}{4}) + \frac{3\phi_1}{2}. \tag{34}$$

The extinction coefficient, k, is calculated as a weighted average of the corresponding values for direct and diffuse radiation:

$$k = f_{\text{dir}}k_{\text{direct}} + (1 - f_{\text{dir}})k_{\text{diffuse}}. \tag{35}$$

From Sellers (1985),

$$k_{\text{direct}} = \frac{G(\mu)}{\mu}(1 - \omega)^{\frac{1}{2}}, \tag{36}$$

where ω is the scattering coefficient. For the diffuse component,

$$k_{\text{diffuse}} = \frac{1}{z_\mu}(1 - \omega)^{\frac{1}{2}}, \tag{37}$$

where z_μ is a pre-calculated parameter derived from an equation within the SiB computer code:

$$z_\mu = \frac{1}{\phi_2}\left(1 - \frac{\phi_1}{\phi_2}\ln\left[\frac{\phi_1 + \phi_2}{\phi_1}\right]\right). \tag{38}$$

Both k_{direct} and k_{diffuse} are forced to lie below $50/L_t$.

For computational efficiency, $(1 - \omega)^{\frac{1}{2}}$ is precomputed by the GCM and sent to the LSM as an input parameter. It varies seasonally due to the dependence of ω on the greenness fraction, f_g:

$$\omega = f_g l_{\text{rt-live}} + (1 - f_g)l_{\text{rt-dead}}, \tag{39}$$

where $l_{\mathrm{rt-live}}$ is the sum of the leaf-element reflectance and leaf-element transmittance for green leaves and $l_{\mathrm{rt-dead}}$ is the corresponding sum for dead (brown) leaves.

Finally, to account for the fact that not all of the leaves are transpiring, the resistance computed with (29) is divided by the greenness fraction, f_g:

$$r_{\mathrm{c-unstressed}} = \frac{r_{\mathrm{c-unstressed,green}}}{f_g}. \tag{40}$$

Thus, a smaller fraction of green leaves leads to a higher canopy resistance.

4.2.2 Environmental Stresses

The unstressed canopy resistance calculated with (29) and (40) is the transpiration resistance used when all environmental conditions are optimal. If conditions are sub-optimal, the resistance increases:

$$r_c = r_{\mathrm{c-unstressed}} F(\mathrm{VPD}) F(T) F(\psi_l), \tag{41}$$

where $F(\mathrm{VPD})$, $F(T)$, and $F(\psi_l)$ are the stress terms (each greater than or equal to 1) associated with vapor pressure deficit, temperature, and leaf water potential, respectively. The stress functions used are largely consistent with those outlined by Jarvis (1976).

a. *Vapor Pressure Deficit Stress.* Early versions of the Mosaic LSM — as well as the version used in the PILPS intercomparison study (Henderson-Sellers et al. 1993) — calculated $F(\mathrm{VPD})$ with

$$\frac{1}{F(\mathrm{VPD})} = \mathrm{Max}\left[0.,\ \ 1. - (e_s(T_c) - e_a) d_{\mathrm{VPD}}\right], \tag{42}$$

where d_{VPD} is a vegetation-specific parameter. A higher vapor pressure deficit, $e_s(T_c) - e_a$, thus leads to a higher value of $F(\mathrm{VPD})$. (The values of T_c and e_a used in (42) are the values from the previous time step, $[T_c]_{\mathrm{old}}$ and $[e_a]_{\mathrm{old}}$.) This formulation differs slightly from that in SiB, which uses a canopy air temperature, T_a, rather than the canopy temperature itself to compute the saturated vapor pressure. In SiB, T_a and T_c can differ due to the imposition of a subcanopy aerodynamic resistance. This resistance is absent in the Mosaic model.

When the Mosaic LSM is coupled to the Aries GCM, however, $F(\mathrm{VPD})$ is set to 1, and thus no vapor pressure deficit stress is allowed. Sensitivity studies (Koster and Suarez 1994) show that when the vapor pressure deficit stress is activated in this coupled system, the near-surface dry bias in the Aries GCM leads to a stress that excessively reduces transpiration. This reduction in the near-surface moisture supply reduces the near-surface vapor pressure even further, and this leads to an even further increase in the vapor pressure deficit stress. This is a positive feedback that can lead to the unrealistic shutdown of transpiration. It must therefore be avoided.

b. *Temperature Stress.* Stomates are assumed to limit transpiration when temperatures are either too high or too low. The equation used by SiB (Sellers et al. 1986) to compute $F(T)$, which is based on the work of Jarvis (1976), has the form:

$$\frac{1}{F(T)_{\mathrm{SiB}}} = h_3(T_c - T_l)(T_h - T_c)^{h_4}, \tag{43}$$

where T_l is the lower temperature limit (below which transpiration ceases), T_h is the upper transpiration limit, and h_3 and h_4 are themselves complicated functions of T_o (the optimum temperature), T_c, and T_h. The Mosaic LSM uses a polynomial approximation to this equation:

$$\frac{1}{F(T)} = \begin{cases} 0 & T_c < T_l \\ (T_c - T_l)(T_c - T_h)(c_1 {T_c}^2 + c_2 T_c + c_3) & T_l < T_c < T_h \\ 0 & T_h < T_c \end{cases} \tag{44}$$

where c_1, c_2, and c_3 are vegetation-specific coefficients that produce an approximation to the more complicated, and more computationally intensive, SiB equations. $[T_c]_{\mathrm{old}}$ is used in (44). Figure 3 shows how well the approximation works for the six vegetation types considered by the Mosaic LSM.

c. *Leaf Water Potential Stress.* Drier soils limit transpiration through the leaf water potential stress. Following SiB, this stress is modeled as

$$\frac{1}{F(\psi_l)} = \begin{cases} 0 & \psi_l < \psi_2 \\ \frac{\psi_l - \psi_2}{\psi_1 - \psi_2} & \psi_2 < \psi_l < \psi_1 \\ 1 & \psi_1 < \psi_l, \end{cases} \tag{45}$$

where ψ_1 is the leaf water potential at which wilting begins and ψ_2 is the leaf water potential at which transpiration is shut down completely.

Equation (45) is difficult to apply directly, however, because ψ_l is itself a function of the transpiration rate, E_T:

$$\psi_l = \psi_r - Z - E_T \frac{r_{\mathrm{plant}} + r_{\mathrm{soil}}}{\rho_w}, \tag{46}$$

where ψ_r is the root-zone moisture potential, Z is the height of the canopy, r_{plant} is the average resistance to moisture transport imposed by the plant, r_{soil} is the average resistance imposed by the soil and root system, and ρ_w is the density of water. The calculation of $F(\psi_l)$ is therefore based on an estimated transpiration rate, E_{T}^*. Combining (45) and (46) gives:

$$\frac{1}{F(\psi_l)} = \begin{cases} 0 & \psi_l < \psi_2 \\ \frac{\psi_r - Z - E_{\mathrm{T}}^* \frac{r_{\mathrm{plant}} + r_{\mathrm{soil}}}{\rho_w} - \psi_2}{\psi_1 - \psi_2} & \psi_2 < \psi_l < \psi_1 \\ 1 & \psi_1 < \psi_l \end{cases} \tag{47}$$

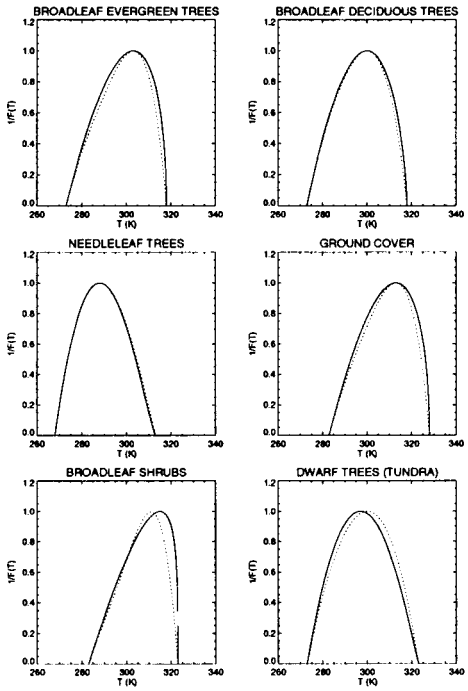

Figure 3: Temperature stress functions ($1/F(T)$) from SiB (solid lines) and the Mosaic LSM (dashed lines) for six vegetation types.

with E_{T}^{*} determined by incorporating (41) and (47) into (25) and then rearranging and solving the resulting equation.

To derive ψ_r, the Mosaic LSM first computes the average degree of saturation in the root zone, $\frac{W_{\mathrm{r}}}{W_{\mathrm{r-sat}}}$, as:

$$\frac{W_{\mathrm{r}}}{W_{\mathrm{r-sat}}} = \frac{W_1 + W_2}{W_{1-\mathrm{sat}} + W_{2-\mathrm{sat}}}, \tag{48}$$

where W_1 and W_2 are the moisture contents in the top and middle soil layers, respectively, and $W_{1-\mathrm{sat}}$ and $W_{2-\mathrm{sat}}$ are the maximum possible moisture contents in these soil layers. This degree of saturation is then employed in (120), an equation that relates moisture potential to soil moisture content, to be discussed later in the context of groundwater diffusion.

The values of ψ_1, ψ_2, Z, and r_{plant} are vegetation-specific and constant. Only r_{soil} varies with the root-zone moisture state. As in SiB, the Mosaic LSM computes

$$r_{\mathrm{soil}} = r_{\mathrm{s1}} + \frac{r_{\mathrm{s2}}}{K}, \tag{49}$$

where K is the average hydraulic conductivity in the root zone, calculated with (48) and (121). The coefficients r_{s1} and r_{s2} are precomputed with:

$$r_{\mathrm{s1}} = \frac{R}{D_d z_d} \tag{50}$$

and

$$r_{s2} = \frac{\alpha_f}{z_d}, \tag{51}$$

where R is the resistance per unit root length, D_d is the root length density, z_d is the rooting depth, and

$$\alpha_f = \frac{1}{8\pi D_d}\left[V_r - 3 - 2\ln\left(\frac{V_r}{1-V_r}\right)\right], \tag{52}$$

where V_r is the volume of root per unit volume of soil. Seasonal variations in V_r result from seasonal variations in D_d:

$$V_r = D_d A_r, \tag{53}$$

where A_r is the average cross-sectional area of a root.

4.3 Resistance for Bare Soil Evaporation

Bare soil evaporation, E_{bs}, is assumed to occur in parallel with transpiration and is effectively calculated with:

$$E_{bs} = \frac{\rho\epsilon}{p_s}\frac{e_s(T_c) - e_a}{r_{bs}}, \tag{54}$$

where r_{bs} is the total resistance to bare soil evaporation, calculated with

$$r_{bs} = (r_{surf} + r_{sca}) f_{hum}. \tag{55}$$

Here r_{surf} is the resistance provided by the soil, r_{sca} is the resistance provided by the subcanopy air (i.e., by the air between the soil surface and the canopy air space), and f_{hum} is a humidity factor.

To calculate r_{surf}, the Mosaic LSM uses:

$$r_{surf} = 26 + 6\left(\frac{W_{1-sat}}{W_1}\right)^2, \tag{56}$$

which is an approximation to an equation used in SiB. Thus, r_{surf} increases strongly as the top layer's soil moisture decreases. The calculation of r_{sca} is also an approximation to a more complicated SiB function. The Mosaic LSM uses:

$$r_{sca} = \frac{c_{sca}}{U_2}, \tag{57}$$

where c_{sca} is a vegetation-specific constant and U_2 is the wind speed at the top of the canopy, estimated with

$$U_2 = \frac{U_m}{c_u \kappa}\ln\left(\frac{Z-d}{z_o}\right), \tag{58}$$

where U_m is the wind speed provided by the GCM, κ is the von Karman constant, Z is the canopy height, d is the zero plane displacement height, and z_o is the roughness length. In the PILPS intercomparison study, c_u is calculated with

$$c_u = 8.4 + \frac{\ln\left(\frac{15.}{z_o}\right)}{\kappa}, \tag{59}$$

in accordance with calculations in SiB. When the LSM is coupled to the Aries GCM, a slightly different calculation is used:

$$c_u = \frac{\ln\left(\frac{50.}{z_o}\right)}{\kappa}. \tag{60}$$

The humidity factor, f_{hum}, accounts for the subsaturated relative humidity, h, within the soil pores. Rather than following SiB's approach for calculating this humidity, the Mosaic LSM uses a computationally simpler formulation:

$$h = \begin{cases} 2\frac{W_1}{W_{1-\text{sat}}} & \frac{W_1}{W_{1-\text{sat}}} < \frac{1}{2}, \\ 1 & \frac{W_1}{W_{1-\text{sat}}} > \frac{1}{2}. \end{cases} \tag{61}$$

The Mosaic LSM then computes

$$f_{\text{hum}} = \frac{e_s(T_c) - e_a}{h e_s(T_c) - e_a}. \tag{62}$$

The formulation used for h in the Mosaic LSM is highly arbitrary and is in fact an approximation to the SiB formulation for a soil with a high "b" parameter (see (120) and (121)). For the parameter values currently used to describe soils, h is underestimated, and thus r_{bs} is probably overestimated. Given the small importance of bare soil evaporation relative to transpiration, and given the uncertainties associated with all of the terms in (55) through (62), particularly the meaning of "average soil moisture content" over a large area, the overestimation of r_{bs} is not considered an important problem. In fact, given the aforementioned uncertainties, an overestimated r_{bs} allows the Mosaic LSM to "err" on the safe side, i.e., to avoid producing too much bare soil evaporation.

4.4 Canopy Interception and Snow; Effective Surface Resistance

Like most other SVAT schemes, the Mosaic LSM includes a representation of the canopy interception reservoir. During a precipitation event in nature, canopy leaves and ground litter can "intercept" a fraction of the rainwater so that it never reaches the soil surface, and this intercepted, free-standing water evaporates at the potential rate. Evaporation of intercepted water in the model, E_{int}, thus effectively proceeds according to the equation

$$E_{\text{int}} = \frac{\rho\epsilon}{p_s}\frac{(e_s(T_c) - e_m)}{r_a}, \tag{63}$$

where e_m is the vapor pressure in the overlying GCM grid box and r_a is the aerodynamic resistance. Some models, such as SiB (Sellers et al. 1986), also include a special within-canopy aerodynamic resistance in the E_{int} equation to describe the difficulty of transporting water vapor from leaf surfaces to the canopy air space. This resistance is ignored in the Mosaic LSM.

In the Mosaic LSM, (63) applies only to that areal fraction of the canopy interception reservoir assumed to be "filled", i.e., at capacity. A corresponding equation is thus needed in the remaining area, from which transpiration, E_T, and bare soil evaporation, $E_{\rm bs}$, are assumed to occur in parallel. An effective resistance to their sum, $r_{\rm Tbs}$ is computed with

$$r_{\rm Tbs}^{-1} = r_c^{-1} + r_{\rm bs}^{-1}, \tag{64}$$

where r_c and $r_{\rm bs}$ are calculated with (41) and (55), respectively; the sum $E_T + E_{\rm bs}$, or $E_{\rm Tbs}$, can then be computed with

$$E_{\rm Tbs} = \frac{\rho\epsilon}{p_s} \frac{(e_s(T_c) - e_m)}{r_a + r_{\rm Tbs}}. \tag{65}$$

The fraction of the land surface tile from which interception loss occurs is assumed to be $\frac{C}{C_s}$, where C is the amount of moisture in the interception reservoir and C_s is the maximum amount possible. (Thus, at a given point on the surface, the interception reservoir is either completely empty or completely full.) Transpiration and bare soil evaporation occur over the remaining fraction, $1 - \frac{C}{C_s}$. For computational convenience, (63) and (65) can be combined into a single equation for interception loss, bare soil evaporation, and transpiration:

$$E_{\rm surf} = \frac{\rho\epsilon}{p_s} \frac{(e_s(T_c) - e_m)}{r_a + r_{\rm eff}}, \tag{66}$$

where $E_{\rm surf}$ is the total evaporation from the land surface ($= E_{\rm int} + E_T + E_{\rm bs}$) and $r_{\rm eff}$ is an effective resistance that can be used to compute this total evaporation. The Mosaic LSM computes $r_{\rm eff}$ with:

$$r_{\rm eff} = r_{\rm Tbs} \frac{1 - \frac{C}{C_s}}{1 + \frac{C}{C_s}\frac{r_{\rm Tbs}}{r_a}}. \tag{67}$$

This is precisely the value of $r_{\rm eff}$ that satisfies the equation

$$E_{\rm surf} = (1 - \frac{C}{C_s}) E_{\rm Tbs} + \frac{C}{C_s} E_{\rm int}, \tag{68}$$

when $E_{\rm surf}$, $E_{\rm int}$, and $E_{\rm Tbs}$ are determined with (66), (63), and (65). In other words, $r_{\rm eff}$ in (66) is the single resistance that produces the correct net evaporation from the tile, given that potential evaporation occurs in the wetted part of the canopy and that transpiration and bare soil evaporation occur in the dry part of the canopy. The simple form of (66), which is consistent with the Penman-Monteith evaporation formulation (Monteith 1965), is made possible by the use of a single temperature to describe the soil surface, the wetted canopy and the dry canopy.

As indicated in Section 3.2, $r_{\rm eff}$ from (67) is incorporated into (9), the vapor flux equation. Equation (9) also makes use of (8), which is an equivalent form of (66).

When snow is present, the different model versions adjust $r_{\rm eff}$ in different ways. In Versions 1 and 2, the presence of snow automatically leads to a zeroing of $r_{\rm eff}$, and sublimation of snow is the only evaporation considered in the energy balance calculations (see Section 3.1). In Version 3, potential evaporation from snow surfaces is assumed to occur in parallel with

interception loss, bare soil evaporation, and transpiration. Version 3 actually uses a slightly different form of (67):

$$r_{\text{eff}} = r_{\text{Tbs}} \frac{1 - f_{\text{pot}}}{1 + f_{\text{pot}} \frac{r_{\text{Tbs}}}{r_a}}. \tag{69}$$

where f_{pot} is the fraction of the tile experiencing either interception loss or snow sublimation. This fraction is estimated with

$$f_{\text{pot}} = 1 - (1 - f_{\text{snow}})(1 - \frac{C}{C_s}), \tag{70}$$

where f_{snow} is the fraction of the tile assumed to be covered by snow, calculated with

$$f_{\text{snow}} = \frac{S}{S + S_{\text{mid}}} \tag{71}$$

in accordance with (24). Note that (69) reduces to (67) in the absence of snow.

In the case of condensation onto the land surface, i.e., when $[E]_{\text{old}}$ is negative, Versions 1 and 2 reset r_{eff} to zero. Version 3 does the same, except that a small ramping function is used to ensure continuity in r_{eff} as $[E]_{\text{old}}$ goes from negative to positive. In Version 3, for $[E]_{\text{old}}$ smaller (more negative) than a critical value E_{crit}, r_{eff} is set to zero. For $[E]_{\text{old}}$ negative but higher than E_{crit}, r_{eff} is multiplied by the factor $1 - [E]_{\text{old}}/E_{\text{crit}}$.

4.5 Derivatives of Effective Surface Resistance

The terms $\frac{\partial r_{\text{eff}}}{\partial T_c}$ and $\frac{\partial r_{\text{eff}}}{\partial e_a}$ in (9) could, in principle, be computed analytically. In the Mosaic LSM, however, they are calculated with:

$$\frac{\partial r_{\text{eff}}}{\partial T_c} = \frac{1}{\epsilon_T} \left[r_{\text{eff}}([T_c]_{\text{old}} + \epsilon_T, [e_a]_{\text{old}}) - r_{\text{eff}}([T_c]_{\text{old}}, [e_a]_{\text{old}}) \right] \tag{72}$$

and

$$\frac{\partial r_{\text{eff}}}{\partial e_a} = \frac{1}{\epsilon_e} \left[r_{\text{eff}}([T_c]_{\text{old}}, [e_a]_{\text{old}} + \epsilon_e) - r_{\text{eff}}([T_c]_{\text{old}}, [e_a]_{\text{old}}) \right], \tag{73}$$

where ϵ_T and ϵ_e are very small increments of $[T_c]_{\text{old}}$ and $[e_a]_{\text{old}}$, respectively. In other words, the Mosaic LSM artificially increases $[T_c]_{\text{old}}$ and $[e_a]_{\text{old}}$, in turn, and recalculates r_{eff} in order to determine the tendency terms. It then resets $[T_c]_{\text{old}}$ and $[e_a]_{\text{old}}$ back to their original values.

4.6 Linearization of Longwave Radiation

The terms $\left[R^{\uparrow}_{\text{lw}}\right]_{\text{old}}$ and $\left[\frac{dR^{\uparrow}_{\text{lw}}}{dT_c}\right]_{\text{old}}$ in (2) are computed with

$$\left[R^{\uparrow}_{\text{lw}}\right]_{\text{old}} = A_{\text{lw}} + B_{\text{lw}}[T_c]_{\text{old}} \tag{74}$$

and

$$\left[\frac{dR_{\mathrm{lw}}^{\uparrow}}{dT_c}\right]_{\mathrm{old}} = B_{\mathrm{lw}}, \tag{75}$$

where A_{lw} and B_{lw} are provided by the GCM in order to ensure consistency between the atmosphere and land calculations. (The Aries atmospheric radiation calculations also use the linearization in (74).)

For the PILPS intercomparison project, A_{lw} and B_{lw} are computed with

$$B_{\mathrm{lw}} = 4\sigma[T_c]_{\mathrm{old}}^3 \tag{76}$$

and

$$A_{\mathrm{lw}} = \sigma[T_c]_{\mathrm{old}}^4 - B_{\mathrm{lw}}[T_c]_{\mathrm{old}}, \tag{77}$$

where σ is the Stefan-Boltzmann constant. Note that this implies

$$\left[R_{\mathrm{lw}}^{\uparrow}\right]_{\mathrm{old}} = \sigma[T_c]_{\mathrm{old}}^4. \tag{78}$$

4.7 Linearization of Heat Flux to Deep Soil

The formulation for heat flux to the deep soil is taken from SiB (Sellers et al. 1986) and is consistent with the standard force-restore formulation of Deardorff (1978). The force-restore equation can be written as

$$\frac{dc}{\sqrt{2}}\frac{dT_s}{dt} = G + \frac{\omega dc}{\sqrt{2}}(\overline{T} - T_s), \tag{79}$$

where d is the depth over which a diurnal temperature wave is felt, c is the volumetric heat capacity, T_s is the surface temperature, G is the imposed surface heating, ω is the frequency of the diurnal temperature cycle, and $\overline{T}$ is the temperature below the surface that is unaffected by the diurnal temperature cycle. The term $\frac{\omega dc}{\sqrt{2}}(\overline{T} - T_s)$ can be considered the heat flux to or from the deep soil.

Following this model, the Mosaic LSM computes $[G_D]_{\mathrm{old}}$ and $[\frac{dG_D}{dT}]_{\mathrm{old}}$ in (6) as

$$[G_D]_{\mathrm{old}} = -\frac{\omega dc}{\sqrt{2}}[T_d - T_c]_{\mathrm{old}} \tag{80}$$

and

$$\left[\frac{dG_D}{dT_c}\right]_{\mathrm{old}} = \frac{\omega dc}{\sqrt{2}} \tag{81}$$

These values are used in (5) to calculate G_D, for use in (21).

For $C_{\mathrm{H-deep}}$, the deep soil heat capacity, we infer from the equations in Deardorff (1978) that

$$\frac{C_{\mathrm{H-deep}}}{C_H} = 2\sqrt{365\pi}, \tag{82}$$

a ratio that is related to the ratio of the depths of the diurnal and annual temperature waves. This is in one sense a loose interpretation of the Deardorff formulation, since Deardorff forced the deep soil temperature with surface heating (G in (79)) rather than with G_D.

5 Water Balance: Solution Procedure

Each of the five moisture reservoirs within a land surface tile in the Mosaic LSM requires a water balance equation:

a. Canopy interception reservoir.

$$[C]_{\text{new}} = [C]_{\text{old}} + (P + S_{\text{melt}} - E_{\text{int}} - P_T)\Delta t, \tag{83}$$

where

C = moisture in the canopy interception reservoir,
P = rainfall rate,
S_{melt} = snowmelt rate,
E_{int} = evaporation from interception reservoir,
P_T = throughfall rate.
Δt = time step duration,

b. Top soil layer.

$$[W_1]_{\text{new}} = [W_1]_{\text{old}} + (P_T - R_s - E_{\text{bs}} - E_{\text{transp1}} - Q_{12})\Delta t, \tag{84}$$

where

W_1 = moisture in the top soil layer,
R_s = surface runoff rate,
E_{bs} = evaporation from bare soil,
E_{transp1} = water removal via transpiration from top soil layer,
Q_{12} = moisture flux from top soil layer to middle soil layer.

c. Middle soil layer.

$$[W_2]_{\text{new}} = [W_2]_{\text{old}} + (-E_{\text{transp2}} + Q_{12} - Q_{23})\Delta t, \tag{85}$$

where

W_2 = moisture in the middle soil layer,
E_{transp2} = water removal via transpiration from middle soil layer,
Q_{23} = moisture flux from middle soil layer to bottom soil layer.

d. Bottom soil layer.

$$[W_3]_{\text{new}} = [W_3]_{\text{old}} + (Q_{23} - Q_{3\infty})\Delta t \tag{86}$$

where

W_3 = moisture in the bottom soil layer,
$Q_{3\infty}$ = rate of moisture drainage out of the bottom soil layer.

e. Snowpack.

$$[S]_{\text{new}} = [S]_{\text{old}} + (P_S - S_{\text{melt}} - E_{\text{snow}})\Delta t, \tag{87}$$

where

S = water equivalent in the snowpack,

P_S = snowfall rate,

S_{melt} = rate of snowmelt, and

E_{snow} = snow sublimation rate.

Unlike the energy balance equations, the water balance equations are not solved implicitly. The individual terms in these equations are discussed in the next section.

6 Water Balance: Components

The water balance equations, (83) through (87), contain only two terms that are provided by the GCM, namely the precipitation rate, P, and the snowfall rate, P_S. The remaining terms are either prognostic variables or moisture fluxes internal to the land surface tile. The present section describes how these moisture fluxes are computed. The calculation of the throughfall rate, P_T, is presented in Section 6.1, along with some discussion on the difficulties of modeling canopy interception in a GCM. Surface runoff, R_s, is discussed in Section 6.2, and the division of the total evaporation into its component parts (E_{int}, E_{transp1}, E_{transp2}, E_{bs}, and E_{snow}) is discussed in Section 6.3. Sections 6.4 and 6.5 describe groundwater diffusion between the soil layers (Q_{12} and Q_{23}) and drainage out of the soil column ($Q_{3\infty}$), respectively. The snowmelt term, S_{melt}, is discussed in Section 6.6.

6.1 Canopy Interception Reservoir

Two different parameterizations of canopy interception have been used in the Mosaic LSM. That in Version 1 was replaced by an improved parameterization (in Versions 2 and 3) that produces more accurate estimates of interception loss on the global scale. This improvement was deemed necessary given the strong contribution of interception loss to total evaporation in the real world (Shuttleworth 1988, Gash et al. 1980) and the importance of interception loss in defining GCM climatology (Koster and Suarez 1994, Scott et al. 1995). The two parameterizations of interception differ only in the way the reservoir is loaded during precipitation events.

6.1.1 Interception Reservoir Capacity

The interception reservoir capacity, in units of $\frac{kg}{m^2}$, is set equal to $0.1L_t$, where L_t is the leaf area index of the vegetation type being modeled. The capacity thus varies with vegetation type and season. Bare soil and desert soil are assumed to have no interception reservoir. Also, the interception associated with ground litter below a vegetation canopy is not modeled explicitly.

The factor 0.1 is arbitrary but consistent with that used in other LSMs, such as the SiB model of Sellers et al. (1986). In fact, the PILPS intercomparison project (Henderson-Sellers et al. 1993) required land surface modelers to set their interception reservoir capacities to $0.1L_l$.

6.1.2 Precipitation Loading

a. Parameterization Issues. Given a rainwater mass generated by the GCM, an LSM's first job is to determine how much of the rainwater should be added to the interception reservoir. Parameterizing this precipitation loading is difficult because rainfall is rarely uniform over a modeled land surface area. The calculated loading reflects assumptions made about the fractional area coverage, f, of the precipitation, as illustrated in Figure 4. The figure shows a simple model in which precipitation is uniform over the prescribed fraction f and is zero elsewhere. The part of the local precipitation depth that exceeds the local available capacity is assumed to be throughfall, the rainwater that falls through the canopy leaves to the soil surface. Smaller values of f lead to smaller amounts of intercepted water.

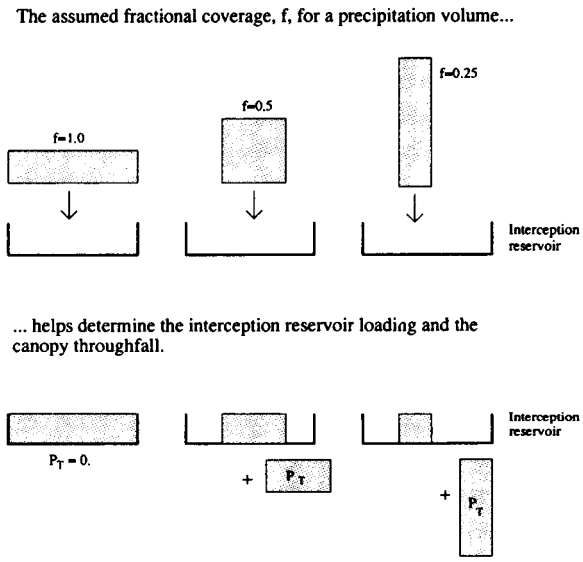

Figure 4: Demonstration of how differences in assumed fractional area coverage of storms can affect the loading of the interception reservoir.

The interception formulations in SiB (Sato et al. 1989; see Appendix C) and some other models use an exponential function rather than an assigned fraction f to describe the subgrid distribution of precipitation. Even so, the same general concepts apply; assuming a steeper exponential function will produce a smaller amount of intercepted water.

While most operational LSMs attempt to characterize the fraction of storm area in a re-

alistic way, very few address the compounding problem of temporal correlation, which is potentially as important but more subtle and difficult. The problem stems from the fact that a simulated storm can span several GCM time steps. Figure 5, for example, shows a storm filling a fraction f of the interception reservoir during time step i. In the next time step, the GCM produces more rainfall, again over the fraction f. The figure shows that the amount of intercepted water calculated during this later time step relies heavily on how (and if) the model redistributes the intercepted moisture from the previous time step. The right side of Figure 5 shows some accounting for memory (temporal correlation) in storm position, whereas the left side does not. The right side clearly produces less interception.

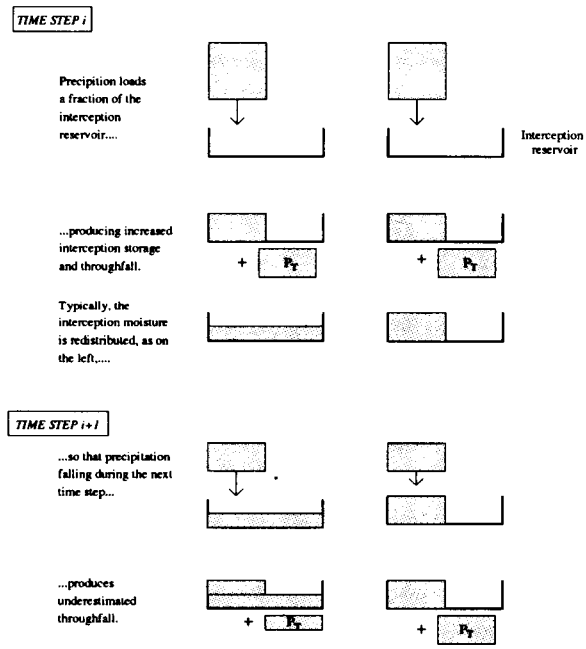

Figure 5: Demonstration that the neglect of temporal correlation in storm position can lead to higher interception storage.

Because typical GCM time steps range from minutes to an hour, and because storms in nature can last much much longer than this, accounting for temporal correlation in storm position is arguably more realistic. If these temporal correlations are ignored, an LSM's behavior can vary with time step length. This is a property to avoid.

In Version 1 of the Mosaic LSM, temporal correlation in storm position is ignored, though not precisely in the way illustrated in Figure 5. Version 2 attempts to account for this correlation with a very simple approximation.

b. Version 1: Uncorrelated Placement of Storms. The Mosaic LSM assumes that precipitation water falls uniformly over a fraction f of the tile, as in Figure 6. The fraction $1 - f$ is not wetted at all, and the precipitation intensity over the fraction f is increased by a factor

$1/f$. In Version 1, f is set to 0.3 for both moist convective precipitation and large scale condensation.

As discussed in Section 4.4, the Mosaic LSM assumes that the interception reservoir is filled in an areal fraction $\frac{C}{C_s}$ of the tile and dry in the areal fraction $1 - \frac{C}{C_s}$. Precipitation, P, is assumed to fall on the *independent* areal fraction f. As shown in Figure 6, this leads to four sub-tile regions. In Region 1, the rain falls on wet leaves and thus immediately falls through the canopy to the soil surface. In Region 3, the rain falls on a dry part of the canopy; the rainwater is added to this part of the interception reservoir until it fills, and the excess water is considered throughfall. Interception calculations are not necessary over Regions 2 and 4. The algorithm supplies a net throughfall and a net increase in canopy interception storage only; the specific moisture state of Region 3, for example, is not remembered between time steps.

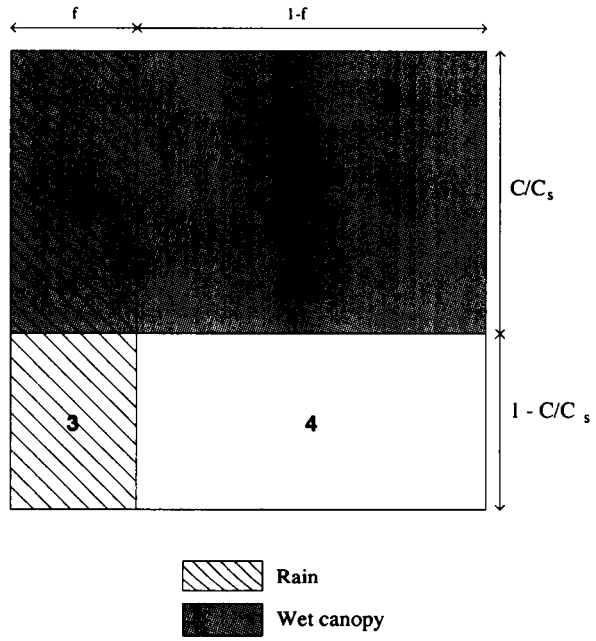

Figure 6: Areal fractions of the tile considered when computing interception of rainwater with Version 1.

In equation form, $P\Delta t$, the precipitation mass (for a tile of unit area), is separated into:

$$P_{\text{dry}} = P\left(1 - \frac{C}{C_s}\right)\Delta t \tag{88}$$

and

$$P_{\text{wet}} = P\frac{C}{C_s}\Delta t, \tag{89}$$

where P_{dry} and P_{wet} are the precipitation masses that fall on the dry and wet leaves, respectively. The maximum amount of rainwater, C_{add}, that can be added to the dry leaves

in Region 3 is

$$C_{\text{add}} = f(C_s - C). \tag{90}$$

The total intercepted moisture is therefore updated with:

$$[C]_{\text{new}} = [C]_{\text{old}} + \text{Min}(P_{\text{dry}}, C_{\text{add}}). \tag{91}$$

The throughfall mass, $P_T \Delta t$, is then calculated with

$$P_T \Delta t = P \Delta t - ([C]_{\text{new}} - [C]_{\text{old}}). \tag{92}$$

c. Versions 2 and 3: Temporal Correlation in Storm Position. The simulated evaporation from the interception reservoir in Version 1, particularly in the tropics, was found to be excessive relative to both the careful point measurements of Shuttleworth (1988) and the global-scale estimates generated by Yale Mintz and Greg Walker (G. Walker, personal communication; see Liston et al. (1993) for a discussion of the estimation procedure). Interception loss is overestimated partly because Version 1 neglects time correlation in storm position. To address this problem, Mosaic LSM Versions 2 and 3 use a simple approximation to time correlation in which part of each time step's rainfall is assumed to fall onto leaves previously wetted by the storm.

In the algorithm, a value is assigned to τ_{storm}, an arbitrary time scale for storm position that must equal or exceed Δt, the time step length. Also, the precipitation falling during a time step is assumed to cover an areal fraction f of the land surface. The precipitation mass is then partitioned into three parts, as indicated in Figure 7. A large fraction, $1 - \frac{\Delta t}{\tau_{\text{storm}}}$, of the rain mass falls onto leaves previously wetted by the storm, as denoted by Region 2 in Figure 7. This rainwater drips through the canopy to the soil surface; it does not add to the interception reservoir's moisture. The remainder of the rainwater falls randomly onto the canopy, part of which is wet (Region 1) and part of which is dry (Region 4). Notice that Regions 1, 2, and 4 together cover the fraction f of the land surface. Also notice that if $\Delta t = \tau_{\text{storm}}$, the area of Region 2 is zero, and all of the rainfall is assigned randomly to the canopy — no temporal memory is imposed.

The precipitation mass, $P \Delta t$, is thus partitioned into three components: the portion falling on the wet Region 2,

$$P_2 = \gamma P \Delta t, \tag{93}$$

the portion falling on the wet Region 1,

$$P_1 = (1 - \gamma) P \frac{C}{C_s} \Delta t, \tag{94}$$

and the portion falling on the dry region 4,

$$P_4 = (1 - \gamma) P \left(1 - \frac{C}{C_s}\right) \Delta t, \tag{95}$$

where γ is calculated with:

$$\gamma = \left(1 - \frac{\Delta t}{\tau_{\text{storm}}}\right). \tag{96}$$

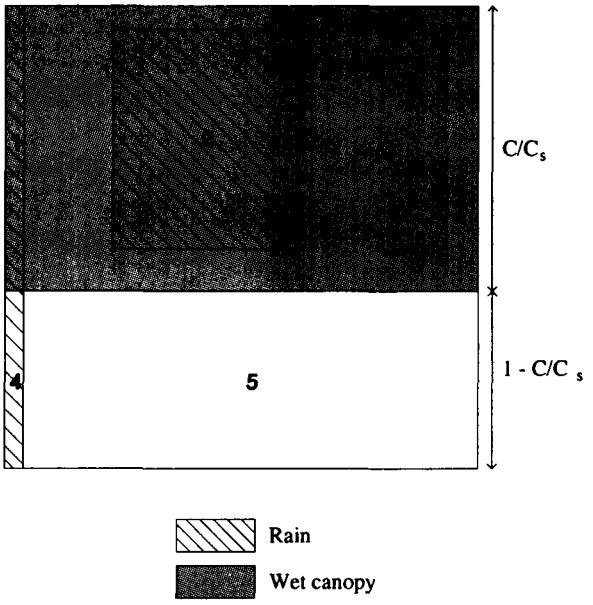

Figure 7: Areal fractions of the tile considered when computing interception of rainwater with Version 2.

Because Δt does not exceed τ_{storm}, γ cannot be negative. Moisture is added to the interception reservoir only in Region 4, which has an available water capacity of

$$C_{\text{add}} = (1-\gamma)f(C_s - C). \tag{97}$$

The interception storage is updated using (91), with P_{dry} replaced with P_4, and throughfall is computed with (92).

These equations are adjusted when necessary to ensure that unrealistic amounts of water do not fall through the canopy at the onset of storms, when the canopy is dry. If the fraction of wetted canopy, $\frac{C}{C_s}$, is less than the assumed storm fraction, f, then γ is recalculated with:

$$\gamma_{\text{adjusted}} = \gamma \frac{C}{C_s}/f. \tag{98}$$

This parameterization differentiates between convective storms, for which f is set to 0.2, and large scale condensation events, for which f is set to 1. The value of τ_{storm} is arbitrarily set to 1 hour.

6.2 Surface Runoff and Infiltration

Infiltration of throughfall into the soil is computed in much the same way as throughfall itself is computed in Version 1.

a. *Versions 1 and 2.* The soil in the areal fraction $\frac{W_1}{W_{1-\text{sat}}}$ of the tile is assumed to be saturated, where W_1 is the moisture content of the top soil layer and $W_{1-\text{sat}}$ is the storage capacity of that layer. The remaining fraction, $1 - \frac{W_1}{W_{1-\text{sat}}}$, is thus assumed to be dry. Throughfall falling onto the saturated area is immediately converted into surface runoff (overland flow), and throughfall falling on the dry fraction must fill the local portion of the top soil layer before it can generate surface runoff. Thus, in analogy with (88) - (92), the throughfall mass falling on the dry fraction, $P_{\text{T-dry}}$, is

$$P_{\text{T-dry}} = P_T \left(1 - \frac{W_1}{W_{1-\text{sat}}}\right) \Delta t. \tag{99}$$

Given that the throughfall covers an areal fraction f of the square, the maximum amount of water that can be added to the soil layer, $W_{1-\text{add}}$, is

$$W_{1-\text{add}} = f(W_{1-\text{sat}} - W_1) \tag{100}$$

The total soil moisture in the top layer is therefore updated with:

$$[W_1]_{\text{new}} = [W_1]_{\text{old}} + \text{Min}(P_{\text{T-dry}}, W_{1-\text{add}}) \tag{101}$$

and the total surface runoff mass, $R_s \Delta t$, is

$$R_s \Delta t = P_T \Delta t - ([W_1]_{\text{new}} - [W_1]_{\text{old}}) \tag{102}$$

The areal fraction of storm coverage, f, is assumed to be the same as that used in the canopy interception loading algorithm. Again, Versions 1 and 2 assume different fractions (see Section 6.1).

b. *Version 3.* The formulation of surface runoff in Version 3 is very similar to that in Versions 1 and 2, the only difference being in the assumed saturated fraction of the tile. The tile is divided into two sub-areas, one that is fully saturated and the other containing a degree of saturation, $W_{1-eq}/W_{1-\text{sat}}$, that is in equilibrium with that in the middle soil layer, so that neither upward nor downward moisture diffusion occurs. This formulation is more consistent with that used for groundwater diffusion; the definition of W_{1-eq} is discussed in more detail in Section 6.4, and the areal partitioning of the tile is identical to that shown in Figure 8.

Given the degrees of saturation in the two sub-areas and the fact that the total amount of water is W_1, the saturated fraction, f_{sat}, can be computed with

$$f_{\text{sat}} = \begin{cases} \frac{W_1 - W_{1-\text{eq}}}{W_{1-\text{sat}} - W_{1-\text{eq}}} & W_1 > W_{1-\text{eq}} \\ 0 & W_1 < W_{1-\text{eq}} \end{cases} \tag{103}$$

Thus, if the soil is dry enough, the "saturated fraction" is zero. The throughfall mass falling on the dry fraction is then

$$P_{\text{T-dry}} = P_T (1 - f_{\text{sat}}) \Delta t, \tag{104}$$

and the maximum amount of water that can be added to the soil layer is

$$W_{1-\text{add}} = f(W_{1-\text{sat}} - W_{1-\text{eq}})(1 - f_{\text{sat}}). \tag{105}$$

Equations (101) and (102) are then used to update the soil moisture and compute the surface runoff. As in Version 2, different values of f are used for moist convection and large-scale condensation.

6.3 Evaporation Sink

Evaporation water is drawn from four possible reservoirs: the snowpack, the canopy interception reservoir, and the upper two soil layers. In Versions 1 and 2, the presence of snow implies that all evaporation is snow sublimation. In Version 3, all reservoirs can be tapped simultaneously.

a. *Versions 1 and 2.* When snow is absent, evaporation extracts water from the interception reservoir and soil layers using

$$E_{\text{int}} = \text{Min}\left(\frac{C}{\Delta t},\ E\frac{C}{C_s}\frac{r_a + r_{\text{Tbs}}}{r_a + \frac{C}{C_s}r_{\text{Tbs}}} \right) \tag{106}$$

and

$$E_{\text{Tbs}} = E - E_{\text{int}}, \tag{107}$$

where E_{Tbs} is equal to $E_T + E_{\text{bs}}$, the sum of transpiration and bare soil evaporation. This breakdown is consistent with the assumptions behind (68). The Mosaic LSM subsequently separates E_{Tbs} with:

$$E_{\text{bs}} = E_{\text{Tbs}}\frac{r_c}{r_{\text{bs}} + r_c} \tag{108}$$

and

$$E_{\text{T}} = E_{\text{Tbs}}\frac{r_{\text{bs}}}{r_{\text{bs}} + r_c}. \tag{109}$$

The moisture associated with E_{bs} is taken from the top soil layer, whereas that associated with E_{T} is taken from the upper two layers:

$$E_{\text{transp1}} = \frac{E_T W_1}{W_1 + W_2}, \tag{110}$$

and

$$E_{\text{transp2}} = \frac{E_T W_2}{W_1 + W_2}. \tag{111}$$

When evaporation is negative, i.e. when dewfall occurs, it is added uniformly to the interception reservoir. (Snowmelt water is added at the same time.) Any excess water above the interception reservoir's capacity falls uniformly onto the ground surface. Subsequently, the top soil layer is checked for saturation, and any excess water is converted to surface runoff.

When snow is present, only the snow variable is updated:

$$E_{\text{snow}} = E \tag{112}$$

Negative evaporation adds to the snowpack.

An error in the computer code used for Versions 1 and 2 led to the substitution of r_{eff} for r_{Tbs} in (106). Offline integrations with the land surface code (using the PILPS forcing data sets) indicate that this error has a negligible effect (less than 0.5%) on the annual energy and water balances.

b. *Version 3.* Under the assumption that snow sublimation and interception loss both proceed at the potential rate and occur in parallel, the sum $E_{\text{snow}} + E_{\text{int}}$, or E_{pot}, can be calculated, in analogy with (106), as:

$$E_{\text{pot}} = \text{Min}\left(\frac{C+S}{\Delta t},\ E f_{\text{pot}} \frac{r_a + r_{\text{Tbs}}}{r_a + f_{\text{pot}} r_{\text{Tbs}}} \right), \tag{113}$$

where f_{pot} is the areal fraction of the tile undergoing potential evaporation, calculated with (70). The ratio of snow sublimation to total evaporation, $f_{\text{E-snow}}$, in Version 3 is then computed with

$$f_{\text{E-snow}} = \frac{E_{\text{pot}}}{E} \frac{f_{\text{snow}}}{f_{\text{snow}} + \frac{C}{C_s}} \tag{114}$$

where f_{snow} is the areal fraction of snow cover (from (71)) and $\frac{C}{C_s}$ is the areal fraction of wetted interception reservoir. Snow sublimation is then calculated with

$$E_{\text{snow}} = f_{\text{E-snow}} E, \tag{115}$$

allowing the calculation of interception loss as

$$E_{\text{int}} = E_{\text{pot}} - E_{\text{snow}}. \tag{116}$$

The sum of bare soil evaporation and transpiration is computed with

$$E_{\text{Tbs}} = E - E_{\text{pot}}, \tag{117}$$

and (108) through (111) are used to update the soil moisture prognostic variables.

6.4 Groundwater Diffusion

Groundwater diffusion between soil layers is computed using a bulk form of the Richards equation. The downward flow between the middle and bottom soil layers, Q_{23}, is assumed to be proportional to a difference in potential, h:

$$Q_{23} = \rho_w K \frac{h_2 - h_3}{\Delta Z_{23}}, \tag{118}$$

where ρ_w is the density of water, K is the hydraulic conductivity in the upstream layer (i.e., in the middle layer if $h_2 > h_3$), and ΔZ_{23} is the distance between the centers of the soil layers. The hydraulic head, h_i, is the sum of a pressure term and an elevation term:

$$h_i = \psi_i + z_i, \tag{119}$$

where z_i is the elevation of the center of layer i relative to some arbitrary baseline and ψ_i is the pressure head (soil moisture potential) in layer i.

Both ψ_i and K_i in layer i are assumed to vary strongly with the degree of saturation in the soil layer. Following Clapp and Hornberger (1978), the Mosaic LSM computes

$$\psi_i = \psi_s \left(\frac{W_{\mathrm{i}}}{W_{\mathrm{i-sat}}} \right)^{-b} \tag{120}$$

and

$$K_i = K_s \left(\frac{W_{\mathrm{i}}}{W_{\mathrm{i-sat}}} \right)^{2b+3}, \tag{121}$$

where ψ_s and K_s are the pressure head and hydraulic conductivity, respectively, of a saturated soil, and b is a soil parameter related to the pore size distribution index. The values for these parameters (see Table 3) are taken from Rawls et al. (1982).

Some subgrid variability is accounted for in the calculation of moisture diffusion between the top and middle soil layers. For this calculation, the Mosaic LSM first computes $W_{1-\mathrm{eq}}$, the water content that the top layer would need in order to have the same hydraulic head as the middle layer:

$$W_{1-\mathrm{eq}} = \left(\frac{\psi_2 - \Delta Z_{12}}{\psi_s} \right)^{-\frac{1}{b}} W_{1-\mathrm{sat}}. \tag{122}$$

If $W_1 > W_{1-\mathrm{eq}}$, downward flow between the top and middle layers is indicated, and the moisture in the top layer is redistributed into two subregions: one for which hydraulic head is identical to that in the second layer, so that no flow occurs, and a fully saturated region with significant downward flow. This is illustrated in Figure 8. The fractional area over which the downward flux occurs, $f_{\mathrm{Q-down}}$, is

$$f_{\mathrm{Q-down}} = \frac{W_1 - W_{1-\mathrm{eq}}}{W_{1-\mathrm{sat}} - W_{1-\mathrm{eq}}}, \tag{123}$$

which is equivalent to f_{sat} in (103). The downward flux itself is computed with

$$Q_{12} = \rho_w f_{\mathrm{Q-down}} K_s \frac{h_{1-\mathrm{sat}} - h_2}{\Delta Z_{12}}, \tag{124}$$

where $h_{1-\mathrm{sat}}$ is the hydraulic head of the saturated portion of the top layer.

If, however, $W_1 < W_{1-\mathrm{eq}}$, upward flow is indicated, and the Mosaic LSM computes

$$Q_{12} = \rho_w K_2 \frac{h_1 - h_2}{\Delta Z_{12}}, \tag{125}$$

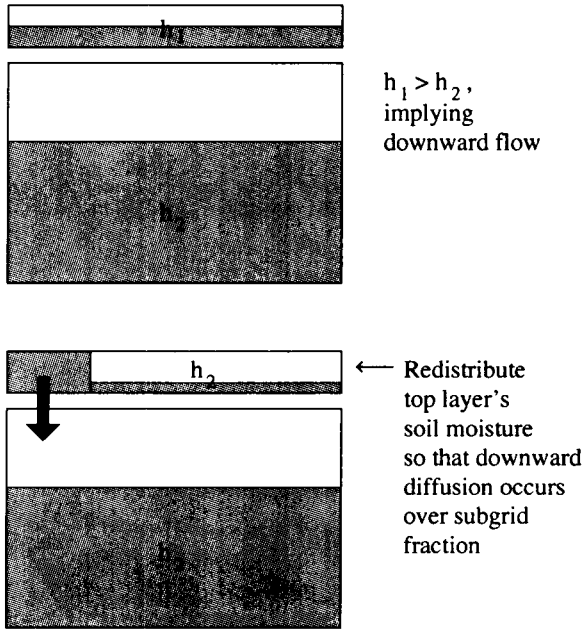

Figure 8: Subgrid distribution of soil moisture assumed for diffusion between top two soil layers.

in analogy with (118).

Limitations on Q_{12} and Q_{23} go beyond simple checks on water availability in the upstream layer and storage availability in the downstream layer. To avoid stability problems, the absolute value of the flow volume, $|Q_{12}\Delta t|$, is forced to remain at or below ΔW, where

$$\Delta W = \frac{1}{2}|W_1 - W_{1-\mathrm{eq}}|. \tag{126}$$

This prevents a large flow volume that would lead to a reversed flow direction in the following time step. A similar limitation is placed on $|Q_{23}\Delta t|$; $W_{2-\mathrm{eq}}$ is computed in analogy to $W_{1-\mathrm{eq}}$, and $|Q_{23}\Delta t|$ is forced to lie at or below $\frac{1}{2}|W_2 - W_{2-\mathrm{eq}}|$. Both Q_{12} and Q_{23} are set to zero if the surface temperature, T_c, lies at or below the freezing point.

6.5 Percolation to the Water Table

Percolation of water out the bottom of the lowest soil layer, $Q_{3\infty}$, is also computed with a bulk form of the Richards equation. The vertical gradient of pressure head, however, is assumed to be zero; only gravitational drainage operates. Furthermore, the presence of bedrock is allowed to reduce the flow. The Mosaic LSM computes:

$$Q_{3\infty} = \rho_w K_3 \cos(\theta), \tag{127}$$

where $\cos(\theta)$ is the cosine of the bedrock angle. If the bedrock is assumed to be far below the lowest soil layer, $\cos(\theta)$ is set to 1.

6.6 Snow Budget

The melting of snow as part of the surface energy balance is treated above in Section 3.4. If, however, the surface temperature already exceeds 0C *when the snow falls*, the snow melts immediately and the ground cools accordingly:

$$S_{\text{melt}} = \text{Min}\left(\; P_S \Delta t, \;\; \frac{([T_c]_{\text{old}} - T_f) C_H}{\lambda_f} \; \right) \qquad \text{for } T_c > T_f \tag{128}$$

and

$$[T_c]_{\text{new}} = [T_c]_{\text{old}} - \frac{S_{\text{melt}} \lambda_f}{C_H} \tag{129}$$

Snowmelt thus proceeds until all snow is depleted or until the ground temperature is reduced to 0C, whichever comes first. The melted snow is added to any rain falling during the time step before the calculation of canopy interception.

If snow is present when rain falls on the surface, the rain water does not "freeze" onto the snow. The snowpack is simply ignored while the rain water is partitioned into canopy interception, infiltration, and surface runoff.

7 Connection to the GCM

Sections 2 through 6 of this report describe the Mosaic LSM's calculations within a single land surface tile. The present section describes how the Mosaic LSM, as currently coded, can be connected to a GCM or an offline driver.

The "TILE" subroutine performs the Mosaic LSM calculations simultaneously for any chosen number, NCH, of land surface tiles. (The calculations performed for one tile, of course, do not affect those performed for another.) The subroutine requires several arrays of dimension NCH as input and produces several arrays of dimension NCH as output, with the nth element in each array corresponding to the nth tile considered. The input arrays hold the forcing variables, certain vegetation parameters, and the states of the prognostic variables (which will be updated within the subroutine). The output arrays hold the diagnostic quantities. Sections 7.1 through 7.3 describe the inputs and outputs of the subroutine in detail.

The geographical locations of the tiles examined in a single call to TILE are not constrained. The tiles need not, for example, reside within the same grid square; all that is required is a means of mapping tile quantities and GCM forcing variables into consistent one-dimensional arrays. An example of such a mapping is illustrated in Figure 9. In the example, a different

leaf area index (LAI) is assigned to each tile, but precipitation is computed in the GCM on a grid square basis. Thus, some repitition of precipitation data is required in the construction of the one-dimensional array of precipitation forcing.

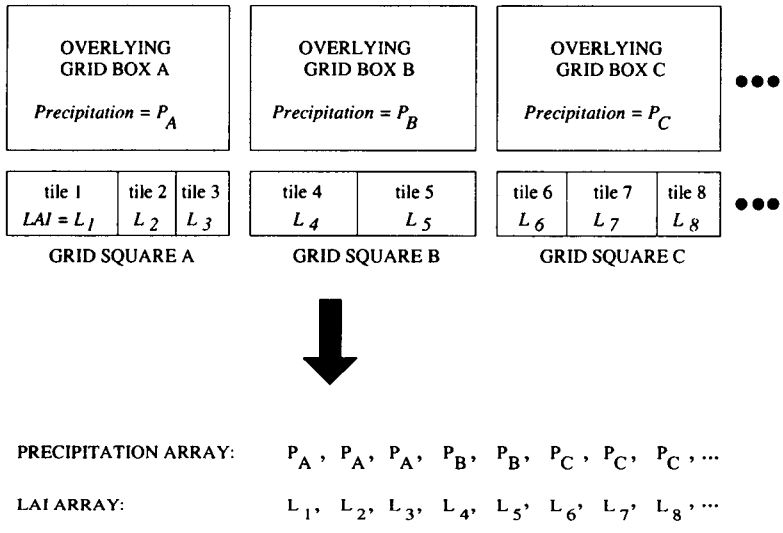

Figure 9: Example of the construction of input arrays for the TILE subroutine.

The subroutine contains no common blocks. It satisfies the conditions for plug-compatibility described by Kalnay et al. (1989).

7.1 Version 1

Version 1 of the Mosaic LSM requires the following inputs (listed by their FORTRAN names) from the GCM at every time step. All quantities are in MKS units. Some of the equations requiring these quantities are indicated in brackets.

All quantities (except for NCH, the number of tiles, and DTSTEP, the time step length) are arrays of dimension NCH.

NCH : The number of tiles processed during the current call to the TILE subroutine. (dimensionless)

DTSTEP : The length of the time step, in seconds. (s) [Δt in (6), (106)]

ITYP : The surface "type", where

1 = Broadleaf evergreen trees.

2 = Broadleaf deciduous trees.

3 = Needle-leaf trees.

4 = Grassland (ground-cover).

5 = Broadleaf shrubs.

6 = Dwarf trees (tundra).

7 = Bare soil.

8 = Desert soil.

TRAIN : The rainfall rate ($\frac{kg}{m^2 s}$). [P in (88), (89)]

TSNOW : The snowfall rate ($\frac{kg}{m^2 s}$). [P_S in (87)]

UM : The wind speed in the overlying GCM grid box ($\frac{m}{s}$). [U_m in (58)]

ETURB : Evaporation rate computed by the GCM using previous time step's T_c and e_a ($\frac{W}{m^2}$). [This is immediately divided by λ to produce $[E]_{\text{old}}$ in (4).]

DEDQA : Derivative of evaporation rate with respect to specific humidity, computed by the GCM using the previous time step's T_c and e_a. ($\frac{W}{m^2}$) [This is immediately multiplied by $\epsilon/(p_s\lambda)$ to convert it to $\left[\frac{\partial E}{\partial e_a}\right]_{\text{old}}$ in (4), (9).]

DEDTC : Derivative of evaporation rate with respect to surface temperature, computed by the GCM using the previous time step's T_c and e_a. ($\frac{W}{m^2 K}$) [This is immediately divided by λ to convert it to $\left[\frac{\partial E}{\partial T_c}\right]_{\text{old}}$ in (4), (9).]

HSTURB : Sensible heat flux computed by the GCM using the previous time step's T_c and e_a. ($\frac{W}{m^2}$). [$[H]_{\text{old}}$ in (3)]

DHSDQA : Derivative of sensible heat flux with respect to specific humidity, computed by the GCM using the previous time step's T_c and e_a. ($\frac{W}{m^2}$) [This is immediately multiplied by ϵ/p_s to convert it to $\left[\frac{\partial H}{\partial e_a}\right]_{\text{old}}$ in (3).]

DHSDTC : Derivative of sensible heat flux with respect to surface temperature, computed by the GCM using the previous time step's T_c and e_a. ($\frac{W}{m^2 K}$) [$\left[\frac{\partial H}{\partial T_c}\right]_{\text{old}}$ in (3)]

TM : The temperature in the overlying GCM grid box. (K) [Not currently used in the Mosaic LSM.]

QM : The specific humidity in the overlying GCM grid box. This is immediately multiplied by p_s/ϵ to produce e_m, the vapor pressure in the overlying grid box. (dimensionless) [Used for certain modifications to energy balance calculations]

CD : Drag coefficient. Its inverse is immediately divided by U_m to produce the aerodynamic resistance, r_a. (dimensionless) [(67)]

SUNANG : The cosine of the solar zenith angle. (dimensionless) [μ in (26)]

PARDIR : The direct component of the photosynthetically active radiation. ($\frac{W}{m^2}$) [Used to compute f_{dir} in (30)]

PARDIF : The diffuse component of the photosynthetically active radiation. ($\frac{W}{m^2}$) [Used to compute $f_{\rm dir}$ in (30)]

SWNET : The net solar radiation absorbed by the surface. This is in fact computed with (22). It appears in TILE's argument list because up to now, calls to the albedo subroutine have taken place outside the calls to the main TILE subroutine. ($\frac{W}{m^2}$) [$R_{\rm sw-net}$ in (6)]

HLWDWN : The downwelling longwave radiation flux. ($\frac{W}{m^2}$) [$R^{\downarrow}_{\rm lw}$ in (6)]

PSUR : Surface pressure, p_s. (mb) [Used to compute air density via perfect gas law and to convert specific humidities into vapor pressures.]

ZLAI : Leaf area index. (dimensionless) [L_t in (26)]

GREEN : Greenness fraction. (dimensionless) [f_g in (40)]

Z2 : Height of canopy leaves. (m) [Z in (46)]

SQSCAT : $\sqrt{1-\omega}$, where ω is the scattering coefficient. (dimensionless) [(36), (37)]

RSOIL1 : The ratio $\frac{R}{D_d z_d}$, where R is the resistance per unit root length, D_d is the root density, and z_d is the rooting depth. ($\frac{s}{m}$) [$r_{\rm s1}$ in [(49)]

RSOIL2 : The ratio $\frac{\alpha_f}{z_d}$, where z_d is the rooting depth and α_f is defined by (52). (dimensionless) [$r_{\rm s2}$ in (49)]

RDC : Term used to compute subcanopy aerodynamic resistance. (dimensionless) [$c_{\rm sca}$ in (57)]

U2FAC : The combination $\frac{1}{c_u \kappa}\ln\left(\frac{Z-d}{z_o}\right)$, where κ is the von Karman constant, Z is the canopy height, d is the zero plane displacement height, z_o is the roughness length, and c_u is calculated with (59) or (60). (dimensionless) [(58)]

QSATTC : The saturated specific humidity at the previous time step's value of T_c. This is immediately multiplied by p_s/ϵ to produce the corresponding saturated vapor pressure, $e_s(T_c)$. (dimensionless) [(8)]

DQSDTC : The derivative of the saturated specific humidity with respect to temperature, evaluated at the previous time step's value of T_c. This is immediately multiplied by p_s/ϵ to produce the corresponding derivative of saturated vapor pressure with respect to temperature, $\frac{\partial e_s}{\partial T_c}$. ($K^{-1}$) [(9)]

ALWRAD : First term in the longwave radiation linearization. ($\frac{W}{m^2}$) [$A_{\rm lw}$ in (74)]

BLWRAD : Second term in the longwave radiation linearization. ($\frac{W}{m^2 K}$) [$B_{\rm lw}$ in (74)]

The Mosaic LSM uses these inputs to update eight prognostic variables:

TC : T_c, the surface and canopy temperature. (K)

TD : T_d, the deep soil temperature. (K)

QA : The specific humidity in the canopy air, computed by multiplying the vapor pressure in the canopy air, e_a, by ϵ/p_s. (dimensionless)

SWET1 : The degree of saturation in the top soil layer, equal to $W_1/W_{1-\text{sat}}$. (dimensionless)

SWET2 : The degree of saturation in the middle soil layer, equal to $W_2/W_{2-\text{sat}}$. (dimensionless)

SWET3 : The degree of saturation in the bottom soil layer, equal to $W_3/W_{3-\text{sat}}$. (dimensionless)

CAPAC : C, the amount of water contained in the canopy interception reservoir. $(\frac{kg}{m^2})$

SNOW : S, the amount of snow water equivalent present. $(\frac{kg}{m^2})$

Version 1 of the Mosaic LSM also produces several model diagnostics:

EVAP : The evaporation rate in $\frac{W}{m^2}$, calculated by multiplying E by λ_e or λ_s, depending on the absence or presence of snow.

SHFLUX : H, the sensible heat flux. $(\frac{W}{m^2})$

RUNOFF : The total runoff generated (sum of R_s and $Q_{3\infty}$). $(\frac{kg}{m^2 s})$

BOMB : Debugging diagnostic. (Not currently used.)

EINT : The interception loss in $\frac{W}{m^2}$, calculated by multiplying E_{int} by λ_e.

ESOI : The evaporation rate from bare soil in $\frac{W}{m^2}$, calculated by multiplying E_{bs} by λ_e.

EVEG : The transpiration rate in $\frac{W}{m^2}$, calculated by multiplying E_T by λ_e.

ESNO : The evaporation rate from snowpack in $\frac{W}{m^2}$, calculated by multiplying E_{snow} by λ_s.

STRDG1 : Special diagnostic. (Not currently used.)

STRDG2 : Special diagnostic. (Not currently used.)

STRDG3 : Special diagnostic. (Not currently used.)

STRDG4 : Special diagnostic. (Not currently used.)

7.2 Version 2

Version 2 of the Mosaic LSM has the same inputs and outputs as Version 1 except for the TRAIN input variable, which is separated for Version 2 into two input variables:

TRAINC : The convective rainfall rate ($\frac{kg}{m^2 s}$). [P in (93), (94), (95); interception and surface runoff algorithms are performed separately for moist convective and large-scale precipitation]

TRAINL : The large-scale rainfall rate ($\frac{kg}{m^2 s}$). [P in (93), (94), (95); interception and surface runoff algorithms are performed separately for moist convective and large-scale precipitation]

7.3 Version 3

Version 3 has the same inputs and outputs as Version 2 except for the modification of the definitions of certain inputs and the addition of several diagnostic outputs. The newly defined inputs are:

ETURB : Evaporation rate computed by the GCM using previous time step's T_c and e_a, now provided in $\frac{kg}{m^2 s}$.

DEDQA : Derivative of evaporation rate with respect to specific humidity, computed by the GCM using the previous time step's T_c and e_a and now provided in $\frac{kg}{m^2 s}$. This is immediately multiplied by ϵ/p_s to produce $\left[\frac{\partial E}{\partial e_a}\right]_{\text{old}}$.

DEDTC : Derivative of evaporation rate with respect to surface temperature, computed by the GCM using the previous time step's T_c and e_a and now provided in $\frac{kg}{m^2 s K}$.

The new diagnostic outputs are:

SMELT : S_{melt}, the rate of snowmelt. ($\frac{kg}{m^2 s}$)

HLATN : $\lambda_s E_{\text{snow}} + \lambda_\epsilon (E_{\text{int}} + E_{\text{T}} + E_{\text{bs}})$, the latent heat flux. ($\frac{W}{m^2}$)

HLWUP : $R^{\uparrow}_{\text{lw}}$, the outgoing longwave radiation flux. ($\frac{W}{m^2}$)

GDRAIN : Q_{23}, the diffusion of moisture across the bottom of the root zone (middle soil layer). ($\frac{kg}{m^2 s}$)

RUNSRF : R_s, the overland flow. ($\frac{kg}{m^2 s}$)

FWSOIL : $P_T - R_s$, the infiltration of rainwater into the top soil layer. ($\frac{kg}{m^2 s}$)

Appendix 1: List of Symbols

A_{lw}	Coefficient used in the linearization of outgoing longwave radiation. $(kg\ s^{-3})$
A_r	Average cross-sectional area of a root. (m^2)
a	Stomatal resistance parameter. $(kg\ m^{-1}s^{-2})$
B_{lw}	Coefficient used in the linearization of outgoing longwave radiation. $(kg\ s^{-3}K^{-1})$
b	Stomatal resistance parameter. $(kg\ s^{-3})$
b	Soil parameter related to pore size distribution index. (dimensionless)
C	Amount of moisture in the canopy interception reservoir. $(kg\ m^{-2})$
C_{add}	Amount of precipitation water that can be added to the interception reservoir during a time step. $(kg\ m^{-2})$
C_H	Heat capacity associated with the surface/canopy system. $(kg\ s^{-2}K^{-1})$
C_s	Maximum amount of water that can be stored in the canopy interception reservoir. $(kg\ m^{-2})$
$C_{\text{H-deep}}$	Heat capacity associated with deep soil. $(kg\ s^{-2}K^{-1})$
c	Stomatal resistance parameter. $(m^{-1}s)$
c	Volumetric heat capacity of soil, for use in force-restore formulation. $(kg\ m^{-1}s^{-2}K^{-1})$
c_{sca}	Vegetation specific constant used to determine subcanopy aerodynamic resistance. (dimensionless)
c_u	Wind profile parameter. (dimensionless)
c_1	Coefficient in temperature stress equation. (K^{-4})
c_2	Coefficient in temperature stress equation. (K^{-3})
c_3	Coefficient in temperature stress equation. (K^{-2})
D_d	Root length density. (m^{-2})
d	Stomatal resistance term. (dimensionless)
d	Zero plane displacement height. (m)
d	Depth over which diurnal wave is felt in force-restore formulation. (m)
d_{VPD}	Parameter controlling vapor pressure deficit stress. (mb^{-1})
E	Evaporation rate. $(kg\ m^{-2}s^{-1})$
E_{bs}	Evaporation rate from bare soil. $(kg\ m^{-2}s^{-1})$
E_{H}	Harmonic mean of E_{surf} and the evaporation flux between the canopy air and the atmosphere, calculated using old values of T_c and e_a. $(kg\ m^{-2}s^{-1})$
E_{int}	Evaporation rate from the interception reservoir. $(kg\ m^{-2}s^{-1})$
E_{pot}	Sum of the evaporation rates from the interception reservoir and the snowpack. $(kg\ m^{-2}s^{-1})$
E_{surf}	Evaporation rate from the ground and canopy surfaces into the canopy air. $(kg\ m^{-2}s^{-1})$
E_{snow}	Evaporation rate from the snowpack. $(kg\ m^{-2}s^{-1})$
E_T	Transpiration rate. $(kg\ m^{-2}s^{-1})$
E_{Tbs}	Sum of transpiration and bare soil evaporation. $(kg\ m^{-2}s^{-1})$
E_{transp1}	Water removal via transpiration from top soil layer. $(kg\ m^{-2}s^{-1})$
E_{transp2}	Water removal via transpiration from middle soil layer. $(kg\ m^{-2}s^{-1})$
e_a	Vapor pressure in the canopy air. (mb)

e_m	Vapor pressure in the air overlying the canopy (*e.g.*, in the lowest GCM layer). (mb)
e_s	Saturated vapor pressure. (mb)
$F(T)$	Factor by which canopy resistance increases due to temperature stress. (dimensionless)
$F(\text{VPD})$	Factor by which canopy resistance increases due to vapor pressure deficit stress. (dimensionless)
$F(\psi_l)$	Factor by which canopy resistance increases due to leaf water potential stress. (dimensionless)
F_o	Flux of photosynthetically active radiation, or PAR. ($kg\ s^{-3}$)
f	Fractional coverage of precipitation. (dimensionless)
f_{dir}	Ratio of direct solar radiation to total solar radiation. (dimensionless)
$f_{\text{E}-\text{snow}}$	Ratio of the snow sublimation mass flux to the total evaporation mass flux. (dimensionless)
f_{hum}	Relative humidity factor that increases resistance to bare soil evaporation. (dimensionless)
f_g	Fraction of leaves that are green. (dimensionless)
f_{pot}	Areal fraction of the tile experiencing interception loss or snow sublimation. (dimensionless)
$f_{\text{Q}-\text{down}}$	Areal fraction of the tile over which downward moisture diffusion occurs between top and middle soil layers. (dimensionless)
f_{sat}	Areal fraction of the tile in which the top soil layer is saturated. (dimensionless)
f_{snow}	Areal fraction of the tile covered by snow. (dimensionless)
G_D	Heat flux to the deep soil. ($kg\ s^{-3}$)
$G(\mu)$	Relative projected area of leaf elements in the direction of the solar zenith angle. (dimensionless)
H	Sensible heat flux into the atmosphere. ($kg\ s^{-3}$)
h	Relative humidity in the soil pores. (dimensionless)
h_i	Hydraulic head in layer i. (m)
$h_{\text{l}-\text{sat}}$	Hydraulic head of the saturated portion of the top soil layer. (m)
K	Hydraulic conductivity of the soil. (ms^{-1})
K_i	Hydraulic conductivity of soil layer i. (ms^{-1})
K_s	Hydraulic conductivity of the soil at saturation. (ms^{-1})
k	Extinction coefficient. (dimensionless)
k_{diffuse}	Extinction coefficient for diffuse radiation. (dimensionless)
k_{direct}	Extinction coefficient for direct radiation. (dimensionless)
L_l	Leaf area index. (dimensionless)
$l_{\text{rt}-\text{dead}}$	Sum of leaf-element reflectance and leaf-element transmittance for dead leaves. (dimensionless)
$l_{\text{rt}-\text{live}}$	Sum of leaf-element reflectance and leaf-element transmittance for green leaves. (dimensionless)

P	Rainfall rate. $(kg\ m^{-2}s^{-1})$
P_{dry}	Rainfall mass falling onto the dry fraction of the canopy. $(kg\ m^{-2})$
P_S	Snowfall rate. $(kg\ m^{-2}s^{-1})$
P_T	Rate of rain throughfall from the canopy leaves to the soil surface. $(kg\ m^{-2}s^{-1})$
$P_{\text{T-dry}}$	Throughfall mass falling onto dry soil. $(kg\ m^{-2})$
P_{wet}	Rainfall mass falling onto the wet fraction of the canopy. $(kg\ m^{-2})$
P_{i}	Rainfall rate onto region i. $(kg\ m^{-2}s^{-1})$
p_s	Surface pressure. (mb)
Q_{12}	Moisture diffusion flux from top soil layer to middle soil layer. $(kg\ m^{-2}s^{-1})$
Q_{23}	Moisture diffusion flux from middle soil layer to lowest soil layer. $(kg\ m^{-2}s^{-1})$
$Q_{3\infty}$	Moisture diffusion flux out the bottom of the lowest soil layer. $(kg\ m^{-2}s^{-1})$
R	Resistance to moisture transport per unit root length. $(m^{-1}s)$
R_s	Surface runoff rate. $(kg\ m^{-2}s^{-1})$
$R_{\text{sw-net}}$	Net shortwave radiation absorbed at the surface. $(kg\ s^{-3})$
$R_{\text{lw}}^{\downarrow}$	Longwave radiation absorbed at the land surface. $(kg\ s^{-3})$
$R_{\text{lw}}^{\uparrow}$	Upward longwave radiation from the land surface. $(kg\ s^{-3})$
$R_{\text{ni-dif}}$	Near-infrared diffuse radiation flux. $(kg\ s^{-3})$
$R_{\text{ni-dir}}$	Near-infrared direct radiation flux. $(kg\ s^{-3})$
$R_{\text{v-dif}}$	Visible diffuse radiation flux. $(kg\ s^{-3})$
$R_{\text{v-dir}}$	Visible direct radiation flux. $(kg\ s^{-3})$
r_a	Aerodynamic resistance. $(m^{-1}s)$
r_{bs}	Resistance to bare soil evaporation. $(m^{-1}s)$
r_c	Canopy resistance to transpiration. $(m^{-1}s)$
$r_{\text{c-unstressed}}$	Unstressed canopy resistance to transpiration. $(m^{-1}s)$
$r_{\text{c-unstressed,green}}$	Unstressed resistance in green leaf fraction of canopy to transpiration. $(m^{-1}s)$
r_{eff}	Effective resistance to the sum of transpiration, bare soil evaporation, interception loss, and snow sublimation. $(m^{-1}s)$
r_{plant}	Average resistance to moisture transport within the vegetation itself. (s)
r_{sca}	Resistance provided by subcanopy air to bare soil evaporation. $(m^{-1}s)$
r_{soil}	Resistance imposed by the soil and root system to moisture transport. (s)
r_{surf}	Resistance provided by the soil itself to bare soil evaporation. $(m^{-1}s)$
r_{s1}	Coefficient used in the calculation of r_{soil}. (s)
r_{s2}	Coefficient used in the calculation of r_{soil}. (m)
r_{Tbs}	Effective resistance to the sum of transpiration and bare soil evaporation. $(m^{-1}s)$
S	Water equivalent in the snowpack. $(kg\ m^{-2})$

S_{crit1}	Snow water equivalent below which snow does not modify albedo. $(kg\ m^{-2})$
S_{crit2}	Snow water equivalent above which only snow albedo is considered. $(kg\ m^{-2})$
S_{melt}	Snowmelt rate. $(kg\ m^{-2}s^{-1})$
S_{mid}	Snow water equivalent for which snow and snow-free areas contribute equally to albedo. $(kg\ m^{-2})$
T_c	Temperature of the surface/canopy system. (K)
T_d	Temperature deep in the soil. (K)
T_f	Freezing point of water. (K)
T_h	Temperature above which temperature stress prevents transpiration. (K)
T_l	Temperature below which temperature stress prevents transpiration. (K)
U_m	Wind speed in the overlying air (*e.g.*, in the lowest GCM grid box). (ms^{-1})
U_2	Canopy air wind speed used in subcanopy aerodynamic resistance calculation. (ms^{-1})
V_r	Volume of root per unit volume of soil. (dimensionless)
W_{avail}	Moisture available during a time step for evaporation. $(kg\ m^{-2})$
W_{i}	Moisture in soil layer i. $(kg\ m^{-2})$
$W_{\text{i-sat}}$	Moisture holding capacity of soil layer i. $(kg\ m^{-2})$
W_{r}	Moisture in the root zone (top layer plus middle layer). $(kg\ m^{-2})$
$W_{\text{r-sat}}$	Moisture holding capacity of the root zone. $(kg\ m^{-2})$
W_1	Moisture in the top soil layer. $(kg\ m^{-2})$
$W_{1-\text{add}}$	Maximum amount of precipitation water that can be added to the top soil layer during a time step. $(kg\ m^{-2})$
$W_{1-\text{eq}}$	Water content in the top soil layer that would be in equilibrium (according to Richards equation) with the water content in the middle soil layer. $(kg\ m^{-2})$
W_2	Moisture in the middle soil layer. $(kg\ m^{-2})$
W_3	Moisture in the bottom soil layer. $(kg\ m^{-2})$
Z	Height of the canopy. (m)
z_d	Rooting depth. (m)
z_i	Elevation (relative to some baseline) of the center of layer i. (m)
z_o	Roughness length. (m)
z_μ	Parameter used in computing extinction coefficient for diffuse radiation. (dimensionless)
α_f	Parameter used in computing resistance to moisture transport in the soil. (m^2)
$\alpha_{\text{ni-dif}}$	Albedo for near-infrared diffuse radiation. (dimensionless)
$\alpha_{\text{ni-dir}}$	Albedo for near-infrared direct radiation. (dimensionless)
$\alpha_{\text{snow,v-dir}}$	Snow albedo for visible direct radiation. (dimensionless)
$\alpha_{\text{v-dif}}$	Albedo for visible diffuse radiation. (dimensionless)
$\alpha_{\text{v-dir}}$	Albedo for visible direct radiation. (dimensionless)
$\alpha_{\text{veg,v-dir}}$	Snow-free albedo for visible direct radiation. (dimensionless)

γ The fraction of a precipitation mass assigned to the storm's previous position. (dimensionless)

Δt Time step length. (s)

ΔW Maximum amount of water that can diffuse between soil layers. $(kg\ m^{-2})$

ΔZ_{12} Distance between the centers of the top and middle soil layers. (m)

ΔZ_{23} Distance between the centers of the middle and bottom soil layers. (m)

δe_a Change in the canopy air vapor pressure, e_a, over the time step. $(kg\ m^{-1}s^{-2})$

δT_c Change in the surface-canopy temperature, T_c, over the time step. (K)

ϵ Ratio of the molecular weight of water vapor to that of dry air. (dimensionless)

ϵ_e Increment in e_a used to compute $\frac{\partial r_{\text{eff}}}{\partial e_a}$. $(kg\ m^{-1}s^{-2})$

ϵ_T Increment in T_c used to compute $\frac{\partial r_{\text{eff}}}{\partial T_c}$. (K)

θ Bedrock slope. (dimensionless)

κ The von Karman constant. (dimensionless)

λ Latent heat of vaporization. (m^2s^{-2})

λ_e Latent heat of vaporization of liquid water. (m^2s^{-2})

λ_f Latent heat of fusion. (m^2s^{-2})

λ_s Latent heat of vaporization of ice (sublimation). (m^2s^{-2})

μ Cosine of the solar zenith angle. (dimensionless)

ρ Density of air. $(kg\ m^{-3})$

ρ_w Density of liquid water. $(kg\ m^{-3})$ ·

σ Stefan-Boltzmann constant. $(kg\ s^{-3}K^{-4})$

τ_{storm} Time scale of storm position. (s)

ϕ_1 Parameter used in computing $G(\mu)$. (dimensionless)

ϕ_2 Parameter used in computing $G(\mu)$. (dimensionless)

χ_L Parameter describing the departure of leaf angles from a spherical distribution. (dimensionless)

Ψ Weighted average of $G(\mu)/\mu$ and Ψ_{dif}. (dimensionless)

Ψ_{dif} A function for diffuse radiation corresponding to the function $G(\mu)/\mu$ for direct radiation. (dimensionless)

ψ_i Soil moisture potential in layer i. (m)

ψ_l Leaf water potential. (m)

ψ_r Soil moisture potential in the root zone (the top and middle soil layers). (m)

ψ_s Soil moisture potential of a saturated soil. (m)

ψ_1 Soil moisture potential above which the vegetation is not moisture-stressed. (m)

ψ_2 Soil moisture potential below which transpiration ceases due to wilting. (m)

ω Scattering coefficient. (dimensionless)

ω Frequency of the diurnal temperature cycle. (s^{-1})

Appendix 2: Tables of Parameter Values

The following tables list the parameter values used for the different land surface types in the Mosaic LSM. Many of these values are stored in data statements in the TILE subroutine; others are either passed down directly to the subroutine in the CALL statement or are used to construct composite variables that are then passed down to the subroutine. Most of the parameter values were derived from values used within SiB biomes (*e.g.*, Dorman and Sellers 1989).

The tables also indicate representative equations in the text that use the parameters.

Parameter	Units	1. Broadleaf evergreen trees	2. Broadleaf deciduous trees	3. Needle-leaf trees	4. Grass-land
C_H (6)	$\frac{kg}{s^2-K}$	70000.	70000.	70000.	70000.
$C_{\mathrm{H-deep}}$ (21)	$\frac{kg}{s^2-K}$	4.74E6	4.74E6	4.74E6	4.74E6
$\frac{\omega dc}{\sqrt{2}}$ (80)	$\frac{kg}{s^3-K}$	5.09	5.09	5.09	5.09
λ_ϵ (7)	$\frac{m^2}{s^2}$	2.4548E6	2.4548E6	2.4548E6	2.4548E6
λ_s (7)	$\frac{m^2}{s^2}$	2.8368E6	2.8368E6	2.8368E6	2.8368E6
λ_f (129)	$\frac{m^2}{s^2}$	3.8200E5	3.8200E5	3.8200E5	3.8200E5
T_f (128)	K	273.16	273.16	273.16	273.16
χ_L (32)	(-)	0.1	0.25	0.01	-0.3
$l_{\mathrm{rt-live}}$ (39)	(-)	0.15	0.15	0.12	0.175
$l_{\mathrm{rt-dead}}$ (39)	(-)	0.161	0.161	0.161	0.58
a (27)	$\frac{kg}{ms^2}$	2335.9	9802.2	2869.7	2582.0
b (27)	$\frac{kg}{s^3}$	0.0	10.6	3.7	1.1
c (27)	$\frac{s}{m}$	153.5	180.0	233.0	110.0

Parameter	Units	5. Broadleaf shrubs	6. Dwarf trees	7. Bare soil	8. Desert soil
C_H	$\frac{kg}{s^2-K}$	70000.	70000.	70000.	70000.
$C_{\mathrm{H-deep}}$	$\frac{kg}{s^2-K}$	4.74E6	4.74E6	4.74E6	4.74E6
$\frac{\omega dc}{\sqrt{2}}$	$\frac{kg}{s^3-K}$	5.09	5.09	5.09	5.09
λ_e	$\frac{m^2}{s^2}$	2.4548E6	2.4548E6	2.4548E6	2.4548E6
λ_s	$\frac{m^2}{s^2}$	2.8368E6	2.8368E6	2.8368E6	2.8368E6
λ_f	$\frac{m^2}{s^2}$	3.8200E5	3.8200E5	3.8200E5	3.8200E5
T_f	K	273.16	273.16	273.16	273.16
χ_L	(-)	0.01	0.20	0.0	0.0
$l_{\mathrm{rt-live}}$	(-)	0.15	0.15	0.002	0.002
$l_{\mathrm{rt-dead}}$	(-)	0.161	0.161	0.002	0.002
a	$\frac{kg}{ms^2}$	93989.4	9802.2	0.0	0.0
b	$\frac{kg}{s^3}$	0.01	10.6	0.0	0.0
c	$\frac{s}{m}$	855.0	180.0	1.0	1.0

Table 1: Heat storage and unstressed canopy resistance parameter values assigned to the eight fundamental surface types. A relevant equation is provided in parentheses.

Parameter	Units	1. Broadleaf evergreen trees	2. Broadleaf deciduous trees	3. Needle-leaf trees	4. Grass-land
d_{VPD} (42)	$\frac{ms^2}{kg}$	0.0273	0.0357	0.0310	0.0238
T_l (44)	K	273.	273.	268.	283.
T_h (44)	K	318.	318.	313.	328.
c_1 (44)	$\frac{1}{K^4}$	-1.43549E-06	-6.83584E-07	1.67699E-07	-1.43465E-06
c_2 (44)	$\frac{1}{K^3}$	7.95859E-04	3.72064E-04	-7.65944E-05	8.24060E-04
c_3 (44)	$\frac{1}{K^2}$	-1.11575E-01	-5.21533E-02	6.14960E-03	-1.19602E-01
A_r (53)	m^2	3.84E-07	3.84E-07	3.84E-07	3.84E-07
z_d (50)	m	1.00	1.00	0.50	0.50
R (50)	$\frac{s}{m}$	7.5E12	7.5E12	7.5E12	4.0E12
ψ_1 (45)	m	-100.	-190.	-200.	-120.
ψ_2 (45)	m	-500.	-250.	-250.	-230.
Z (46)	m	35.	20.	17.	0.6
r_{plant} (46)	$\frac{s}{m}$	2.45E08	2.45E08	2.45E08	2.50E08
Parameter	Units	5. Broadleaf shrubs	6. Dwarf trees	7. Bare soil	8. Desert soil
d_{VPD}	$\frac{ms^2}{kg}$	0.0275	0.0275	0.0	0.0
T_l	K	283.	273.	0.0	0.0
T_h	K	323.	323.	0.0	0.0
c_1	$\frac{1}{K^4}$	-2.76097E-06	-1.58094E-07	0.0	0.0
c_2	$\frac{1}{K^3}$	1.57617E-03	8.44847E-05	0.0	0.0
c_3	$\frac{1}{K^2}$	-2.26109E-01	-1.27272E-02	0.0	0.0
A_r	m^2	3.84E-07	3.84E-07	1.0E-07	1.0E-07
z_d	m	0.50	0.20	0.10	0.10
R	$\frac{s}{m}$	7.5E12	7.5E12	1.E12	1.E12
ψ_1	m	-200.	-200.	-200.	-10.
ψ_2	m	-400.	-400.	-250.	-100.
Z	m	5.	0.6	0.1	0.1
r_{plant}	$\frac{s}{m}$	2.50E08	2.50E08	2.45E08	1E08

Table 2: Parameter values related to environmental stress factors, for each of the eight fundamental surface types. A relevant equation is provided in parentheses.

Parameter	Units	1. Broadleaf evergreen trees	2. Broadleaf deciduous trees	3. Needle-leaf trees	4. Grass-land
$W_{1-\text{sat}}$ (120)	$\frac{kg}{m^2}$	8.4	8.4	8.4	8.4
$W_{2-\text{sat}}$ (120)	$\frac{kg}{m^2}$	621.6	621.6	621.6	197.4
$W_{3-\text{sat}}$ (120)	$\frac{kg}{m^2}$	840.0	840.0	840.0	420.0
Top layer ΔZ (124)	m	0.02	0.02	0.02	0.02
Middle layer ΔZ (118)	m	1.48	1.48	1.48	0.47
Bottom layer ΔZ (118)	m	2.00	2.00	2.00	1.00
K_s (121)	$\frac{m}{s}$	1.2E-06	1.2E-06	1.2E-06	1.2E-06
ψ_s (120)	m	-.281	-.281	-.281	-.281
b (120)	(-)	4.	4.	4.	4.
cosθ (127)	(-)	0.1736	0.1736	0.1736	0.1736
Parameter	Units	5. Broadleaf shrubs	6. Dwarf trees	7. Bare soil	8. Desert soil
$W_{1-\text{sat}}$	$\frac{kg}{m^2}$	8.704	8.4	4.	4.
$W_{2-\text{sat}}$	$\frac{kg}{m^2}$	204.5	71.4	4.	4.
$W_{3-\text{sat}}$	$\frac{kg}{m^2}$	435.2	420.0	130.56	130.56
Top layer ΔZ	m	0.02	0.02	0.0092	0.0092
Middle layer ΔZ	m	0.47	0.17	0.0092	0.0092
Bottom layer ΔZ	m	1.00	1.00	0.30	0.30
K_s	$\frac{m}{s}$	5.83E-05	1.2E-06	1.2E-06	5.83E-05
ψ_s	m	-.073	-.281	-.281	-.073
Soil parameter b	(-)	1.69	4.	4.	1.69
cosθ	(-)	1.00	0.1736	0.1736	1.00

Table 3: Water balance parameter values assigned to the eight fundamental surface types. A relevant equation is provided in parentheses. ΔZ refers to the thickness of a soil layer.

Parameter	Units	1. Broadleaf evergreen trees	2. Broadleaf deciduous trees	3. Needle-leaf trees	4. Grass-land
$\alpha_{\text{veg,v-dir}}$ (23)	(-)	See KS91	See KS91	See KS91	See KS91
$\alpha_{\text{veg,v-dif}}$ (23)	(-)	See KS91	See KS91	See KS91	See KS91
$\alpha_{\text{veg,ni-dir}}$ (23)	(-)	See KS91	See KS91	See KS91	See KS91
$\alpha_{\text{veg,ni-dif}}$ (23)	(-)	See KS91	See KS91	See KS91	See KS91
S_{crit1}, corrected (23)	$\frac{kg}{m^2}$	5.	5.	5.	5.
S_{crit2}, corrected (23)	$\frac{kg}{m^2}$	25.	25.	25.	25.
$\alpha_{\text{snow,v-dir}}$, Ver. 1 (23)	(-)	0.50	0.50	0.50	0.70
$\alpha_{\text{snow,v-dif}}$, Ver. 1 (23)	(-)	0.50	0.50	0.50	0.70
$\alpha_{\text{snow,ni-dir}}$, Ver. 1 (23)	(-)	0.50	0.50	0.50	0.70
$\alpha_{\text{snow,ni-dif}}$, Ver. 1 (23)	(-)	0.50	0.50	0.50	0.70
S_{mid} (71)	$\frac{kg}{m^2}$	50.	50.	50.	2.
$\alpha_{\text{snow,v-dir}}$, Ver. 3 (24)	(-)	0.85	0.85	0.85	0.85
$\alpha_{\text{snow,v-dif}}$, Ver. 3 (24)	(-)	0.85	0.85	0.85	0.85
$\alpha_{\text{snow,ni-dir}}$, Ver. 3 (24)	(-)	0.50	0.50	0.50	0.50
$\alpha_{\text{snow,ni-dif}}$, Ver. 3 (24)	(-)	0.50	0.50	0.50	0.50
Parameter	Units	5. Broadleaf shrubs	6. Dwarf trees	7. Bare soil	8. Desert soil
$\alpha_{\text{veg,v-dir}}$	(-)	See KS91	See KS91	0.1	0.3
$\alpha_{\text{veg,v-dif}}$	(-)	See KS91	See KS91	0.1	0.3
$\alpha_{\text{veg,ni-dir}}$	(-)	See KS91	See KS91	0.2	0.35
$\alpha_{\text{veg,ni-dif}}$	(-)	See KS91	See KS91	0.2	0.35
S_{crit1}, corrected	$\frac{kg}{m^2}$	5.	5.	5.	5.
S_{crit2}, corrected	$\frac{kg}{m^2}$	25.	25.	25.	25.
$\alpha_{\text{snow,v-dir}}$, Ver. 1	(-)	0.60	0.60	0.70	0.70
$\alpha_{\text{snow,v-dif}}$, Ver. 1	(-)	0.60	0.60	0.70	0.70
$\alpha_{\text{snow,ni-dir}}$, Ver. 1	(-)	0.60	0.60	0.70	0.70
$\alpha_{\text{snow,ni-dif}}$, Ver. 1	(-)	0.60	0.60	0.70	0.70
S_{mid}	$\frac{kg}{m^2}$	50.	2.	2.	2.
$\alpha_{\text{snow,v-dir}}$, Ver. 3	(-)	0.85	0.85	0.85	0.85
$\alpha_{\text{snow,v-dif}}$, Ver. 3	(-)	0.85	0.85	0.85	0.85
$\alpha_{\text{snow,ni-dir}}$, Ver. 3	(-)	0.50	0.50	0.50	0.50
$\alpha_{\text{snow,ni-dif}}$, Ver. 3	(-)	0.50	0.50	0.50	0.50

Table 4: Reflectance parameters. A relevant equation is provided in parentheses. KS91 refers to *Koster and Suarez* [1991].

Month	1. Broadleaf evergreen trees	2. Broadleaf deciduous trees	3. Needle-leaf trees	4. Grass-land
January	5.117	0.520	8.760	0.782
February	5.117	0.520	9.160	0.893
March	5.117	0.867	9.827	1.004
April	5.117	2.107	10.093	1.116
May	5.117	4.507	10.360	1.782
June	5.117	6.773	10.760	3.671
July	5.117	7.173	10.493	4.782
August	5.117	6.507	10.227	4.227
September	5.117	5.040	10.093	2.004
October	5.117	2.173	9.827	1.227
November	5.117	0.867	9.160	1.004
December	5.117	0.520	8.760	0.893

Month	5. Broadleaf shrubs	6. Dwarf trees	7. Bare soil	8. Desert soil
January	3.760	0.739	0.001	0.001
February	3.760	0.739	0.001	0.001
March	2.760	0.739	0.001	0.001
April	1.760	0.739	0.001	0.001
May	1.760	0.739	0.001	0.001
June	1.760	1.072	0.001	0.001
July	1.760	5.072	0.001	0.001
August	5.760	5.739	0.001	0.001
September	10.760	4.405	0.001	0.001
October	7.760	0.739	0.001	0.001
November	4.760	0.739	0.001	0.001
December	3.760	0.739	0.001	0.001

Table 5: Seasonal variation of leaf area index, L_l (dimensionless).

Month	1. Broadleaf evergreen trees	2. Broadleaf deciduous trees	3. Needle-leaf trees	4. Grass-land
January	0.905	0.026	0.913	0.568
February	0.905	0.026	0.917	0.622
March	0.905	0.415	0.923	0.664
April	0.905	0.759	0.925	0.697
May	0.905	0.888	0.927	0.810
June	0.905	0.925	0.905	0.908
July	0.905	0.836	0.902	0.813
August	0.905	0.697	0.913	0.394
September	0.905	0.331	0.898	0.443
October	0.905	0.166	0.855	0.543
November	0.905	0.015	0.873	0.553
December	0.905	0.026	0.913	0.498

Month	5. Broadleaf shrubs	6. Dwarf trees	7. Bare soil	8. Desert soil
January	0.798	0.451	0.001	0.001
February	0.532	0.451	0.001	0.001
March	0.362	0.451	0.001	0.001
April	0.568	0.451	0.001	0.001
May	0.568	0.451	0.001	0.001
June	0.568	0.622	0.001	0.001
July	0.568	0.920	0.001	0.001
August	0.868	0.697	0.001	0.001
September	0.651	0.076	0.001	0.001
October	0.515	0.451	0.001	0.001
November	0.630	0.451	0.001	0.001
December	0.798	0.451	0.001	0.001

Table 6: Seasonal variation of greenness fraction, f_g (dimensionless).

Month	1. Broadleaf evergreen trees	2. Broadleaf deciduous trees	3. Needle-leaf trees	4. Grass-land
January	2.653	0.52	1.112	0.0777
February	2.653	0.52	1.103	0.0778
March	2.653	0.666	1.088	0.0778
April	2.653	0.910	1.082	0.0779
May	2.653	1.031	1.076	0.0778
June	2.653	1.044	1.068	0.0771
July	2.653	1.042	1.073	0.0759
August	2.653	1.037	1.079	0.0766
September	2.653	1.036	1.082	0.0778
October	2.653	0.917	1.088	0.0779
November	2.653	0.666	1.103	0.0778
December	2.653	0.52	1.112	0.0778

Month	5. Broadleaf shrubs	6. Dwarf trees	7. Bare soil	8. Desert soil
January	0.245	0.0752	0.0112	0.0112
February	0.245	0.0752	0.0112	0.0112
March	0.227	0.0752	0.0112	0.0112
April	0.200	0.0752	0.0112	0.0112
May	0.200	0.0752	0.0112	0.0112
June	0.200	0.0757	0.0112	0.0112
July	0.200	0.0777	0.0112	0.0112
August	0.267	0.0778	0.0112	0.0112
September	0.292	0.0774	0.0112	0.0112
October	0.280	0.0752	0.0112	0.0112
November	0.258	0.0752	0.0112	0.0112
December	0.245	0.0752	0.0112	0.0112

Table 7: Seasonal variation of roughness length, z_o (m).

Month	1. Broadleaf evergreen trees	2. Broadleaf deciduous trees	3. Needle-leaf trees	4. Grass-land
January	285.87	211.32	565.41	24.43
February	285.87	211.32	587.05	24.63
March	285.87	218.78	623.46	24.80
April	285.87	243.40	638.13	24.96
May	285.87	294.87	652.86	25.72
June	285.87	345.90	675.04	27.74
July	285.87	355.18	660.24	30.06
August	285.87	341.84	645.49	28.86
September	285.87	307.22	638.13	25.90
October	285.87	244.84	623.46	25.11
November	285.87	218.78	587.05	24.80
December	285.87	211.32	565.41	24.63

Month	5. Broadleaf shrubs	6. Dwarf trees	7. Bare soil	8. Desert soil
January	103.60	22.86	23.76	23.76
February	103.60	22.86	23.76	23.76
March	102.35	22.86	23.76	23.76
April	100.72	22.86	23.76	23.76
May	100.72	22.86	23.76	23.76
June	100.72	23.01	23.76	23.76
July	100.72	24.36	23.76	23.76
August	105.30	24.69	23.76	23.76
September	107.94	24.04	23.76	23.76
October	106.59	22.86	23.76	23.76
November	104.49	22.86	23.76	23.76
December	103.60	22.86	23.76	23.76

Table 8: Seasonal variation of c_{sca}. (dimensionless).

Month	1. Broadleaf evergreen trees	2. Broadleaf deciduous trees	3. Needle-leaf trees	4. Grass-land
January	19737.8	5010.	9000.0	5500.
February	19737.8	5010.	9200.0	5625.
March	19737.8	5270.	9533.3	5750.
April	19737.8	6200.	9666.7	5875.
May	19737.8	8000.	9800.0	6625.
June	19737.8	9700.	9866.7	8750.
July	19737.8	9500.	9733.3	9375.
August	19737.8	8400.	9666.7	6875.
September	19737.8	6250.	9533.3	6000.
October	19737.8	5270.	9200.0	5750.
November	19737.8	5010.	9000.0	5625.
December	19737.8	5010.	9000.0	5500.

Month	5. Broadleaf shrubs	6. Dwarf trees	7. Bare soil	8. Desert soil
January	6500.	10625.	1.	1.
February	6000.	10625.	1.	1.
March	5500.	10625.	1.	1.
April	5500.	10625.	1.	1.
May	5500.	10625.	1.	1.
June	5500.	11250.	1.	1.
July	5500.	18750.	1.	1.
August	7500.	17500.	1.	1.
September	8500.	10625.	1.	1.
October	7000.	10625.	1.	1.
November	6500.	10625.	1.	1.
December	6500.	10625.	1.	1.

Table 9: Seasonal variation of root length density, D_d (m^{-2}).

Month	1. Broadleaf evergreen trees	2. Broadleaf deciduous trees	3. Needle-leaf trees	4. Grass-land
January	27.37	13.66	13.76	0.218
February	27.37	13.66	13.80	0.227
March	27.37	14.62	13.86	0.233
April	27.37	15.70	13.88	0.239
May	27.37	16.33	13.90	0.260
June	27.37	16.62	13.93	0.299
July	27.37	16.66	13.91	0.325
August	27.37	16.60	13.89	0.313
September	27.37	16.41	13.88	0.265
October	27.37	15.73	13.86	0.244
November	27.37	14.62	13.80	0.233
December	27.37	13.66	13.76	0.227

Month	5. Broadleaf shrubs	6. Dwarf trees	7. Bare soil	8. Desert soil
January	2.813	0.10629	0.0001	0.0001
February	2.813	0.10629	0.0001	0.0001
March	2.662	0.10629	0.0001	0.0001
April	2.391	0.10629	0.0001	0.0001
May	2.391	0.10629	0.0001	0.0001
June	2.391	0.12299	0.0001	0.0001
July	2.391	0.21521	0.0001	0.0001
August	2.975	0.22897	0.0001	0.0001
September	3.138	0.19961	0.0001	0.0001
October	3.062	0.10629	0.0001	0.0001
November	2.907	0.10629	0.0001	0.0001
December	2.813	0.10629	0.0001	0.0001

Table 10: Seasonal variation of zero plane displacement height, d (m).

References

Clapp, R.B., and G.M. Hornberger, 1978: Empirical equations for some soil hydraulic properties. *Water Resour. Res.*, **14**, 601-604.

Deardorff, J. W., 1978: Efficient prediction of ground surface temperature and moisture, with inclusion of a layer of vegetation. *J. Geophys. Res.*, **83**, 1889-1903.

Dickinson, R. E., A. Henderson-Sellers, P. J. Kennedy, and M. F. Wilson, 1986: Biosphere-atmosphere transfer scheme (BATS) for the NCAR Community Climate Model. *Tech. Note TN-275+STR*, 69 pp., Nat. Cent. for Atmos. Res., Boulder, Colorado.

Dorman, J. L., and P. J. Sellers, 1989: A global climatology of albedo, roughness length and stomatal resistance for atmospheric general circulation models as represented by the Simple Biosphere model (SiB). *J. App. Met.*, **28**, 833-855.

Gash, J. H. C., I. R. Wright, and C. R. Lloyd, 1980: Comparative estimates of interception loss from three coniferous forests in Great Britain. *J. Hydrology*, **48**, 89-105.

Henderson-Sellers, A., Z.-L. Yang, and R. E. Dickinson, 1993: The project for the intercomparison of land surface parameterization schemes (PILPS). *Bull. Amer. Meteor. Soc.*, **74**, 1335-1349.

Jarvis, P., 1976: The interpretation of the variations in leaf water potential and stomatal conductance found in canopies in the field. *Phil. Trans. R. Soc. Lond.*, **273**, 593-610.

Kalnay, E., M. Kanamitsu, J. Pfaendtner, J. Sela, M. Suarez, J. Stackpole, J. Tuccillo, L. Umscheid, and D. Williamson, 1989: Rules for the interchange of physical parameterizations, *Bull. Am Met. Soc.*, **70**, 620-622.

Koster, R., and M. Suarez, 1991: A simplified treatment of SiB's land surface albedo parameterization. *NASA Tech. Memo. 104538*, National Aeronautics and Space Administration, Washington, D.C., 11 pp.

Koster, R., and M. Suarez, 1992a: Modeling the land surface boundary in climate models as a composite of independent vegetation stands. *J. Geophys. Res.*, **97**, 2697-2715.

Koster, R., and M. Suarez, 1992b: A comparative analysis of two land surface heterogeneity representations. *J. Climate*, **5**, 1379-1390.

Koster, R., and M. Suarez, 1993: Climate variability studies with a coupled land/atmosphere model. *Macroscale Modelling of the Hydrosphere* (W. B. Wilkinson, ed.), *International Association of Hydrological Sciences Publication 214*, 173-181.

Koster, R., and M. Suarez, 1994: The components of a SVAT scheme and their effects on a GCM's hydrological cycle. *Advances in Water Resources*, **17**, 61-78.

Koster, R., and M. Suarez, 1995: Relative contributions of land and ocean processes to precipitation variability. *Journal of Geophysical Research*, **100**, 13775-13790.

Liston, G.E., Y.C. Sud, and G.K. Walker, 1993: Design of a global soil moisture initialization procedure for the simple biosphere model. *NASA Tech. Memo. 104590*, National Aeronautics and Space Administration, Washington, D.C., 130 pp.

Monteith, J. L., 1965: Evaporation and environment. *Symposium of the Society for Experimental Biology*, **19**, 205-234.

Rawls, W.J., D.L. Brakensiek, and K.E. Saxton, 1982: Estimation of soil water properties. *Transactions of the ASAE*, **25**, 1316-1320 & 1328.

Sato, N., P. Sellers, D. Randall, E. Schneider, J. Shukla, J. Kinter, Y.-T. Hou, and E. Albertazzi, 1989: Implementing the simple biosphere model (SiB) in a general circulation model, Methodologies and results. *NASA Contractor Report 185509*, National Aeronautics and Space Administration, Washington, D.C., 76 pp.

Scott, R., R. Koster, D. Entekhabi, and M. Suarez, 1995: Effect of a canopy interception reservoir on hydrological persistence in a general circulation model. *Journal of Climate*, **8**, 1917-1922.

Scott, R., D. Entekhabi, R. Koster and M. Suarez, submitted: Time scales of land surface evapotranspiration response. *Journal of Climate.*

Sellers, P. J., 1985: Canopy reflectance, photosynthesis and transpiration. *Int. J. Remote Sens.*, **6**, 1335-1372.

Sellers, P. J., Y. Mintz, Y. C. Sud, and A. Dalcher, 1986: A simple biosphere model (SiB) for use within general circulation models. *J. Atmos. Sci.*, **43**, 505-531.

Shuttleworth, W.J., 1988: Evaporation from Amazonian rainforest. *Proc. R. Soc. Lond. B*, **233**, 321-346.

Previous Volumes in This Series

Volume 1 *September 1994*	Documentation of the Goddard Earth Observing System (GEOS) general circulation model - Version 1 **L.L. Takacs, A. Molod, and T. Wang**
Volume 2 *October 1994*	Direct solution of the implicit formulation of fourth order horizontal diffusion for gridpoint models on the sphere **Y. Li, S. Moorthi, and J.R. Bates**
Volume 3 *December 1994*	An efficient thermal infrared radiation parameterization for use in general circulation models **M.-D. Chou and M.J. Suarez**
Volume 4 *January 1995*	Documentation of the Goddard Earth Observing System (GEOS) Data Assimilation System - Version 1 **James Pfaendtner, Stephen Bloom, David Lamich, Michael Seablom, Meta Sienkiewicz, James Stobie, and Arlindo da Silva**
Volume 5 *April 1995*	Documentation of the Aries-GEOS dynamical core: Version 2 **Max J. Suarez and Lawrence L. Takacs**
Volume 6 *April 1995*	A Multiyear Assimilation with the GEOS-1 System: Overview and Results **Siegfried Schubert, Chung-Kyu Park, Chung-Yu Wu, Wayne Higgins, Yelena Kondratyeva, Andrea Molod, Lawrence Takacs, Michael Seablom, and Richard Rood**
Volume 7 *September 1995*	Proceedings of the Workshop on the GEOS-1 Five-Year Assimilation **Siegfried D. Schubert and Richard B. Rood**

Volume 8
March 1996

Documentation of the Tangent Linear Model and Its Adjoint of the Adiabatic Version of the NASA GEOS-1 C-Grid GCM: Version 5.2

Weiyu Yang and I. Michael Navon

REPORT DOCUMENTATION PAGE

Form Approved
OMB No. 0704-0188

1. AGENCY USE ONLY *(Leave blank)*	2. REPORT DATE	3. REPORT TYPE AND DATES COVERED
	March 1996	Technical Memorandum

4. TITLE AND SUBTITLE
Technical Report Series on Global Modeling and Data Assimilation
Volume 9 - Energy and Water Balance Calculations in the Mosaic LSM

5. FUNDING NUMBERS
C - NAS5-32332
Code 974

6. AUTHOR(S)
Randal D. Koster and Max J. Suarez
Max J. Suarez, Editor

7. PERFORMING ORGANIZATION NAME(S) AND ADDRESS (ES)
Hydrological Sciences Branch
Climate and Radiation Branch
Goddard Space Flight Center
Greenbelt, Maryland

8. PEFORMING ORGANIZATION REPORT NUMBER
96B00051

9. SPONSORING / MONITORING ADGENCY NAME(S) AND ADDRESS (ES)
National Aeronautics and Space Administration
Washington, DC 20546-0001

10. SPONSORING / MONITORING ADGENCY REPORT NUMBER
TM-104606, Vol. 9

11. SUPPLEMENTARY NOTES
Koster and Suarez: Goddard Space Flight Center, Greenbelt, MD

12a. DISTRIBUTION / AVAILABILITY STATMENT
Unclassified - Unlimited
Subject Category 46
This publication is available from the NASA Center for AeroSpace Information, 800 Elkridge Landing Road, Linthicum Heights, MD 21090-2934, (301)621-0390.

12b. DISTRIBUTION CODE

13. ABSTRACT *(Maximum 200 words)*

The Mosaic land surface model (LSM), which is designed for use with an atmospheric general circulation model (GCM), computes areally-averaged energy and water fluxes from the land surface in response to meteorological forcing. The model allows explicit vegetation control over the computed surface energy and water balances, with environmental stresses acting to increase canopy resistance and thus decrease transpiration. The scheme includes a canopy interception reservoir and three soil reservoirs: a thin layer near the surface, a middle layer that encompasses the remainder of the root zone, and a lower "recharge" layer for long-term storage. Bare soil evaporation, transpiration, and interception loss occur in parallel, and runoff occurs both as overland flow during precipitation events and as groundwater drainage out of the recharge layer. A complete snow budget is included. The model was originally derived from the SiB model of Sellers et al. (1986) and still maintains certain SiB formulations, particularly those for canopy resistance.

14. SUBJECT TERMS
Land surface models, LSM, atmospheric general circulation model, GCM, surface energy, water balance, environmental stresses, snow budget, SiB model

15. NUMBER OF PAGES
76

16. PRICE CODE

17. SECURITY CLASSIFICATION OF REPORT	18. SECURITY CLASSIFICATION OF THIS PAGE	19. SECURITY CLASSIFICATION OF ABSTRACT	20. LIMITATION OF ABSTRACT
Unclassified	Unclassified	Unclassified	UL